JOURNAL OF GEOPHYSICAL RESEARCH, VOL. 111, E05005, doi:10.1029/2005JE002608, 2006

Are the Earth and the Moon compositionally alike? Inferences on lunar composition and implications for lunar origin and evolution from geophysical modeling

A. Khan,[1,2] J. Maclennan,[3,4] S. R. Taylor,[5,6] and J. A. D. Connolly[7]

Received 16 October 2005; revised 29 December 2005; accepted 9 February 2006; published 27 May 2006.

[1] The main objective of the present study is to discuss in detail the results obtained from an inversion of the Apollo lunar seismic data set, lunar mass, and moment of inertia. We inverted directly for lunar chemical composition and temperature using the model system CaO-FeO-MgO-Al_2O_3-SiO_2. Using Gibbs free energy minimization, stable mineral phases at the temperatures and pressures of interest, their modes and physical properties are calculated. We determine the compositional range of the oxide elements, thermal state, Mg#, mineralogy and physical structure of the lunar interior, as well as constraining core size and density. The results indicate a lunar mantle mineralogy that is dominated by olivine and orthopyroxene (~80 vol%), with the remainder being composed of clinopyroxene and an aluminous phase (plagioclase, spinel, and garnet present in the depth ranges 0–150 km, 150–200 km, and >200 km, respectively). This model is broadly consistent with constraints on mantle mineralogy derived from the experimental and observational study of the phase relationships and trace element compositions of lunar mare basalts and picritic glasses. In particular, by melting a typical model mantle composition using the pMELTS algorithm, we found that a range of batch melts generated from these models have features in common with low Ti mare basalts and picritic glasses. Our results also indicate a bulk lunar composition and Mg# different to that of the Earth's upper mantle, represented by the pyrolite composition. This difference is reflected in a lower bulk lunar Mg# (~0.83). Results also indicate a small iron-like core with a radius around 340 km.

Citation: Khan, A., J. Maclennan, S. R. Taylor, and J. A. D. Connolly (2006), Are the Earth and the Moon compositionally alike? Inferences on lunar composition and implications for lunar origin and evolution from geophysical modeling, *J. Geophys. Res.*, *111*, E05005, doi:10.1029/2005JE002608.

1. Introduction

[2] The Moon so far has not lifted its veil to such a degree that we are in the possession of a detailed picture of how it formed and evolved. While a consensus surrounding lunar formation has emerged, tying its origin to a major collisional episode with the Earth, its subsequent evolution is yet to be fully understood. *Hartmann and Davis* [1975] and *Cameron and Ward* [1976] proposed that the Moon formed as a result of a collision in the late stages of planetary formation between the proto-Earth and an impactor having a substantial fraction of the proto-Earth mass. A fraction of the mantle material ejected by the impact would settle in a ring around the Earth from which the Moon would accrete. Since its inception in the mid-1970s the giant impact model has undergone several variations, although the underlying theme has more or less been the same [e.g., *Cameron*, 2000; *Canup and Asphaug*, 2001; *Canup*, 2004]. Whatever the details, the Moon is to a large extent made from mantle material of the impactor (~80%) which has been subjected to high temperatures. Since it is assumed that the Earth and the impactor had already differentiated into a Fe-core and a silicate mantle, the material ejected from the terrestrial and the impactor mantle has a low iron content which can explain the lunar iron deficiency and, given the unknown chemical make-up of the impactor, any differences in bulk composition between the two bodies. Tying the origin of the Moon to the Earth dates back to *George Darwin* [1881], who sought to explain the difference in density between the two bodies by hypothesizing that the Moon had been spun off the Earth's mantle.

---

[1] Niels Bohr Institute, University of Copenhagen, Denmark.

[2] Formerly at Institut de Physique du Globe de Paris (DGSP), Paris, France.

[3] Department of Earth Sciences, University of Cambridge, Cambridge, UK.

[4] Formerly at School of GeoSciences, University of Edinburgh, Edinburgh, UK.

[5] The Australian National University, Canberra, Australia.

[6] Also at Lunar and Planetary Institute, Houston, Texas, USA.

[7] Earth Sciences Department, Swiss Federal Institute of Technology, Zurich, Switzerland.

0148-0227/06/2005JE002608$09.00

[3] The internal structure and composition of a planet or satellite provide important clues and constraints on theories for how such bodies formed and evolved. For the Moon these issues were addressed when the U.S. Apollo program installed seismometers on the Moon from 1969 to 1972 which collected data continuously until 1977. In spite of the limited amount of information that could be gathered from the lunar seismic data, studies of lunar seismicity and internal structure provided information on the gross lunar structure and led to the picture of the Moon as being a highly differentiated body. Analyses of returned samples then and now corroborate this scenario.

[4] Issues that, in principle, can be addressed geophysically and can potentially constrain lunar formation and evolution include the question of whether the Moon has a metallic iron core, the depth of differentiation needed to produce the plagioclase rich highland crust, its bulk composition and the question of how the Moon is related to the Earth.

[5] However, as seismic velocity profiles only indirectly reflect such important variables as composition and thermal state, it is not possible to make inferences about the latter without making recourse to assumptions. Nonetheless, several interpretations of the seismic velocity profiles acquired in the Apollo era, notably the models by *Goins et al.* [1981] and *Nakamura* [1983], have been undertaken with the goal of constraining its composition [e.g., *Buck and Toksöz*, 1980; *Hood and Jones*, 1987; *Mueller et al.*, 1988; *Kuskov and Kronrod*, 1998]. In wanting to bridge the inherent shortcoming underlying the interpretation of a seismic velocity model rather than the data from which this model has been derived, we chose, in a recent analysis of ours [*Khan et al.*, 2006], to invert the Apollo lunar seismic data set in combination with mass and moment of inertia in order to constrain the mantle composition using the model system CaO-FeO-MgO-Al_2O_3-SiO_2 (CFMAS) and thermal state directly. A knowledge of the latter enables estimation of Mg# (molar MgO/(MgO+FeO)), mineralogical composition, density, *P*- and *S*-wave velocity structure, as well as putting bounds on core size and density, which can all be used to distinguish between different hypotheses of lunar origin [e.g., *Wood*, 1986].

[6] Points that we want to raise in this paper include the question of the need for a transition, that is, a change in chemical composition and/or mineralogy, between the upper and middle mantle, as previous studies seemed to converge upon the need for a positive discontinuous change in seismic velocity and density in the mantle at a depth of about 500 km. Moreover, we will focus on the implications of our bulk lunar compositions and assess to what extent these models can be used to put constraints on lunar origin and evolution. Furthermore, geochemical and petrological observations can be used to investigate the composition and evolution of the lunar interior. Several key features of the compositions of mare basalts and picrite glasses have been used in conjunction with the results of experimental studies of lunar material in order to infer the major element composition and mineralogy of the lunar mantle [*Longhi*, 1992a, 1992b; *Shearer and Papike*, 1993; *Hess*, 1994]. It is therefore important to study the relationship between the results of our compositional models, which fit the geophysical data, and the composition of lunar basalts and picritic glasses. Our aim is to determine whether melting of some of our mantle compositions could produce magma with compositions similar to those of primitive lunar basalts and picrites. As our compositional models only encompass the elements in the CFMAS system, we restricted our comparison to basalts and glasses with low TiO_2 concentrations. In particular we examine major and trace element data from the Apollo 12 and 15 green glasses, the Apollo 12 and 15 olivine normative basalts, and the Apollo 17 very low Ti basalts.

[7] The inverse method employed here is general and provides through the unified description of phase equilibria a way of constructing planetary models where the radial variation of mineralogy and density with pressure and temperature is naturally specified, allowing us to directly invert for chemical composition and temperature. This improves previous attempts to constrain mantle composition which were limited to either forward modeling of a restricted range of compositions and temperature profiles [*Buck and Toksöz*, 1980; *Hood and Jones*, 1987; *Mueller et al.*, 1988]. or inverse modeling using Gibbs free energy minimization [*Kuskov and Kronrod*, 1998], akin to the present approach, although the latter authors do not invert data directly, but only earlier derived seismic velocity profiles.

[8] As the methodology underlying the geophysical inversion is described in detail in the paper by *Khan et al.* [2006], we will presently abstain from reiterating modeling aspects and refer the interested reader to that study. The paper presented here is arranged as follows: Section 2 contains an overview of the composition of the Moon inferred from sample analysis, lunar orbiter missions (Apollo, Clementine and Lunar Prospector) and modeling results, section 3 discusses the geophysical constraints on the thermal state of the lunar interior, section 4 reviews earlier investigations, section 5 describes the geophysical data employed in this study, and section 6 briefly delineates our model and modeling aspects employed here, whereas subsequent sections discuss results and implications.

2. Overview of the Composition of the Moon

2.1. Mg Number of the Moon

[9] The establishment of the bulk Mg and Fe contents of the Moon is difficult on account of the extensive differentiation the Moon is thought to have undergone, following accretion [*Warren*, 1985]. This makes all estimates of the Mg# based on geochemistry, model dependent at best. To complicate the problem, there is no decisive evidence that the Moon possesses a small iron core, although recent investigations strongly favor the existence of a small dense metallic core [*Hood et al.*, 1999; *Williams et al.*, 2001; *Khan et al.*, 2004; *Khan and Mosegaard*, 2005]. The depletion of Fe in the Moon is accompanied by a depletion of all siderophile elements [*Righter and Drake*, 1996] that is correlated with increasing metal-silicate partition coefficients but not with increasing volatility [*Newsom*, 1986; *Righter et al.*, 2000]. This is evidence of metal segregation somewhere, but perhaps this occurred during metal-silicate fractionation in precursor bodies prior to the formation of the Moon, so that this observation neither supports nor negates the presence of a small metallic core in the Moon. This notion is reinforced by the requirement in the Cameron-Benz-Canup models of lunar origin that the im-

pactor had already formed a metallic core. Nevertheless, estimates of the bulk lunar iron content converge around 13 wt% FeO (10.6 wt% Fe), an amount that is needed to satisfy uniquely both the moment of inertia and mass of the Moon [*Mueller et al.*, 1988; *Jones and Hood*, 1990; *Jones and Palme*, 2000]. This Fe value is about 1.5 times higher than the terrestrial mantle value of 6.2 wt% Fe. The terrestrial mantle is enriched in Mg relative to the CI chondrite abundances and the terrestrial Mg# seems well established at about 89 [*Palme and Nickel*, 1985]. For the Moon, various geochemical and petrological estimates from several sources average about 20 wt% Mg [*Lodders and Fegley*, 1998] which for an Fe value of 10.6 wt% give a bulk Moon Mg# of 82, with estimates ranging between 0.80 and 0.85. In these calculations, the interelement ratios of Si, Mg and Al in the Moon have commonly been assumed to be chondritic but there is little evidence for such compositional systematics. The Mg/Si and Al/Si ratios vary widely among the meteorites [*Jarosewich*, 1990] and as noted, the terrestrial mantle differs notably from the canonical CI values [*Drake and Righter*, 2002, Figure 2]. So there is no reason to assume that the impactor, from which most of the Moon is derived [*Canup and Asphaug*, 2001; *Canup*, 2004], had CI interelement ratios for the major elements or specifically a CI Mg/Al ratio [*Jones and Delano*, 1989]. In contrast, estimates based on geophysical calculations [*Kuskov*, 1997; *Kuskov and Kronrod*, 1998] average around 16 wt% Mg, a value that lowers the lunar Mg# to 79. The major conclusion is that the lunar Mg# seems to be perhaps 10 mol% lower than that of the terrestrial mantle, reinforcing the chemical differences between the two bodies and supporting the simulations of the giant impact hypothesis that derives the Moon mostly from the silicate mantle of the impactor.

2.2. Lunar Composition as Inferred From Sample Data

[10] The Moon is depleted in volatile elements relative both to the Earth and to CI. How much of the depletion of the volatile elements was due to early nebular processes and how much has resulted from the Moon-forming collision is problematic [*Taylor*, 2001]. There has been a longstanding controversy over the question whether the Moon is significantly enriched in refractory elements relative to the Earth. The near-surface enrichment of many incompatible elements, possibly concentrated in the residual KREEP from the crystallization of the magma ocean and the presence of a thick highland crust of plagioclase feldspar raise the possibility of a Moon with an enhanced refractory element content relative to CI. The crustal abundance constraint on the bulk lunar composition depends critically on the thickness of the crust, the abundance of anorthite (An96) in the crust and the distribution of KREEP. The average crustal Al_2O_3 content has been calculated at 28.5 wt% [*Wieczorek and Zuber*, 2001] compared to earlier estimates of 24.6 wt% [*Taylor*, 1982]. According to *Lucey et al.* [1995], data from the Clementine Mission established the Al-rich composition of the highland crust, requiring that relative to the Earth, there is an enrichment of refractory elements (e.g., Ca, Al, Ti, REE, U, Th) in the Moon. The plagioclase-rich upper crust extends to 30 km (from central peak data [*Wieczorek and Zuber*, 2001]) so that a thinner crust will increase the relative proportion of the upper crust that is high in Al_2O_3. Many models assume whole-Moon melting, but if the crust is derived from a smaller volume of the Moon, then an increased bulk-Moon abundance of Al_2O_3 is required. Uranium and thorium are refractory elements and so their abundances correlate with those of Al, Ca and Ti in the bulk Moon, unlike the less refractory Si and Mg. The terrestrial U abundance of about 20 ppb [*Ringwood*, 1979; *Taylor*, 1982] is tightly constrained by an interlocking set of isotopic and chemical abundance ratios. The bulk lunar alumina value (6%) estimated by *Taylor* [1982] thus implies a lunar uranium value of 33 ppb, assuming a CI Al/U ratio. On this basis, the value of 6.9 wt% alumina of *Kuskov* [1997] yields a bulk lunar uranium abundance of 38 ppb. On the basis of the K/U ratio, *Drake* [1996] gave a minimum estimate of 27 ppb uranium on the assumption that all the lunar potassium was concentrated in the highland crust. However, enough potassium and uranium must be retained in the deep interior to provide the typical values of 500 ppm potassium and 200 ppb uranium in mare basalts, derived later by partial melting. In addition, much of the potassium and uranium in the Moon ends up being concentrated in the final residual melt from the crystallization of the magma ocean, that is trapped beneath the anorthositic crust so that surface values may be misleading. Although bulk lunar uranium values as low as 19 ppb [*Rasmussen and Warren*, 1985] have been proposed (see next section), these fail to provide enough uranium (or other refractory elements) for geochemically reasonable lunar models (see detailed discussion by *Taylor* [1986]). A basic problem in trying to estimate the bulk lunar abundances of U, Th, K and the other incompatible elements, is that they appear to be concentrated in the Procellarum KREEP Terrane [*Haskin*, 1998; *Jolliff et al.*, 2000; *Korotev*, 2000; *Wieczorek and Philipps*, 2000]. The implication of this segregation under the lunar near-side of the residual melt from the lunar magma ocean is that little information about the bulk Moon abundances for any of these trace elements can be derived either from returned samples or from remote sensing measurements across the lunar surface. Integration of global data and assessment of variations with depth, as might be done from measurements of crater ejecta, are required. The same comment applies to localized measurements of heat flow, unless a major lunar grid is established, or some other technique for establishing the integrated global heat flux is developed [e.g., *Wieczorek and Philipps*, 2000]. Thus geochemical estimates for the abundances of the refractory lithophile trace elements (U, Th, Zr, REE, etc.) may be best constrained by their correlation with the abundance of major refractory elements such as Al and Ca.

3. Geophysical Constraints on the Thermal State of the Moon

[11] As mineral elastic constants are highly temperature dependent any inferences drawn from a seismic velocity model must be subject to prior considerations of possible bounds on the lunar temperature profile. Here we shall consider the constraints that can be placed on the present-day thermal state of the Moon which largely stem from geophysical observations, such as surface heat flow data, gravity data, seismic data and electromagnetic sounding data, although the latter three data sets can only be used indirectly to infer temperature.

[12] The most obvious means to obtain information about the interior thermal state of a planetary body is by direct measurement of its heat flow. For the Moon such measurements have been conducted, but were unfortunately only undertaken at two sites, obtaining heat flow values of 21 ± 3 and 14 ± 2 mW/m^2, respectively [*Langseth et al.*, 1976]. Assuming steady state heat flow (current heat production within the Moon equals current heat loss through the surface), Langseth et al. estimated the bulk Moon U concentration to be 46 ppb. The importance of estimating the bulk Moon U content is, as already mentioned, that it can be used as a guide in establishing the overall composition of the Moon. It is generally assumed that the refractory lithophile elements (Al, Ca, Sc, Ti, V, Sr, Y, Zr, Nb, all REEs, Hf, Ta, Th, and U) occur in chondritic proportions to one another in the planets [*Warren and Rasmussen*, 1987]. Further support for this comes from the compositional trends among lunar rocks [*Warren and Kallemeyn*, 1984]. The major refractory elements, Al and Ca, can therefore be directly estimated from the U and Th content. However, the nonuniform distribution of KREEP, that contains most of the lunar budget of these elements, adds considerable uncertainty to such calculations.

[13] The high U content and by implication the other refractory elements, has usually been taken as evidence for a refractory-rich Moon [*Taylor*, 1982]. *Warren and Rasmussen* [1987], however, argue that the estimated heat flow at the two sites is too high by a factor of roughly 1.15–1.2. Owing to the different megaregolith thicknesses over the highlands and the mare, coupled with the unusually low conductivity of the megaregolith, it has been suggested that a heat flow focusing effect would occur along the highlands/mare boundaries, which are representative of the locales where the measurements were made [*Conel and Morton*, 1975; *Rasmussen and Warren*, 1985]. Readjusting for this effect and furthermore, to match geophysically assessed selenotherms [e.g., *Pullan and Lambeck*, 1980; *Hood et al.*, 1982a, 1982b], *Warren and Rasmussen* [1987], obtain a global averaged heat flow of 12 mW/m^2 and a bulk Moon U content of 14–21 ppb, questioning the enhanced refractory nature of the Moon (see *Taylor et al.* [2006] for further discussion). Depending on the U concentration, the latter authors estimate present-day temperatures at a depth of 240 km to be somewhere in the range from 700 to 1100°C.

[14] Further constraints on the temperature of the lunar mantle come from the Apollo lunar seismic data in the form of seismic Q values ($1/Q$ is proportional to the fraction of energy that is dissipated in the lunar interior per loading cycle). The effect of anelasticity on seismic velocity is proportional to the elastic wave attenuation ($1/Q$), if attenuation is small and has weak frequency dependence as is observed in the terrestrial mantle [*Minster*, 1980]. Shear wave attenuation depends on a number of different factors, such as frequency and composition through melting temperature, which itself depends on pressure and absolute temperature. Attenuation as a function of temperature, T, in the mantle has been considered by many [e.g., *Karato*, 1993] to be in the form of an exponential relation $Q \propto \exp(1/T)$. Owing to the dependence of Q on the other parameters, the estimated Q values [*Nakamura and Koyama*, 1982] can only be used to make qualitative statements about the thermal state of the lunar interior. The crustal Q-value (depth range 0–45 km) is around 6000 for both P and S waves and is an order of magnitude greater than the Earth's and is ascribed to the absence of water and volatiles in the Moon [*Latham et al.*, 1970]. The upper mantle Q values (depth range ~45–560 km) are also very high, with values of around 4000–7000 for P-waves and ~4000 for S waves, indicating temperatures well below solidus. Middle mantle Q values (depth range ~560–1100 km) are ~1500 for P waves and suggest increased temperatures. However, these still must lie below the solidus, as this is the region where the deep moonquakes are localized and stresses are accumulated. Going into the lower mantle, quantitative information becomes scarce, although the somewhat abrupt cessation of deep moonquake activity below ~1100 km depth [*Nakamura et al.*, 1973] points toward temperatures approaching or maybe even attaining the solidus. Recent evidence for a molten state of the lunar core [*Williams et al.*, 2001; *Khan et al.*, 2004; *Khan and Mosegaard*, 2005] suggest temperatures exceeding the solidus in the deep lunar interior (quoted Q values are from *Nakamura et al.* [1982]).

[15] The maintenance of mascons over a period of 3 to 4 Gyr can also be used to place certain constraints on the thermal state of the upper mantle. By looking at the gravity anomalies associated with the mascons, *Pullan and Lambeck* [1980] tried to estimate the temperature in the upper mantle. Inversion of gravity data for density anomalies and associated stress state were combined with flow laws determined in the laboratory to estimate strain rates which, together with an estimate of the total strain that the Moon has experienced, provide upper limits on mantle temperatures. The results indicate temperatures of about 800°C at 300 km depth.

[16] A more definitive approach to deduce limits on the lunar thermal profile relies on the geophysical method of electromagnetic sounding. The lunar conductivity profile is obtained from measurements of the inductive response to time-varying external magnetic fields during intervals when the Moon is in the solar wind or terrestrial magnetosheath (see *Sonett* [1982] for a review). Briefly, use is made of time-dependent measurements by a high-altitude orbiting magnetometer to monitor the input field, and a surface magnetometer to monitor the sum of the input and induced fields. Application of this technique yielded bounds on the mantle conductivity profile and an upper bound of ~435 km on the radius of a highly electrically conducting core [*Dyal et al.*, 1976; *Hobbs et al.*, 1983]. Overall, the mantle conductivity was found to continuously increase from the surface down to the center of the Moon. Once the electrical conductivity profile has been established, it can be combined with laboratory measurements of conductivity versus temperature for relevant mineral assemblages to deduce limits on the thermal profile as a function of depth [e.g., *Duba et al.*, 1976; *Huebner et al.*, 1979; *Hood et al.*, 1982a, 1982b]. However, as noted by *Hood* [1986] this approach is limited by a number of factors which include the unknown mantle composition, incomplete laboratory measurements of electrical conductivity for appropriate mineral compositions and not least the uncertainties surrounding the estimated lunar electrical conductivity profile. Electrical conduction is related to temperature through an Arrhenius-type law of the form $\sigma = \Sigma_{n=1}^{3} \sigma_n \exp(-E_n/kT)$, where the

three terms are representative of electronic, ionic and impurity conduction, respectively, *k* is Boltzmann's constant, *T* temperature, E_n activation energy and σ_n is a nearly constant, slowly varying function of temperature. To obtain an idea of the model variability implied by the data, *Hood et al.* [1982b] obtained by forward modeling a suite of conductivity models which produced data responses that were within the 1σ error limit of the measurements. Laboratory measurements were then used to translate the conductivity models into temperature models, which for a 100% pyroxene (containing 6.8 wt % Al_2O_3) model were found to lie in the ranges 200–700°C at 200 km depth, 500–800°C at 500 km depth, 1000–1200°C at 1000 km depth and 1200–1650°C at 1500 km depth.

[17] All the available constraints reviewed above, have been summarized by *Hood and Zuber* [2000] to a temperature profile that starts at 0°C at 0 km depth, increases to ~750°C at 300 km depth, with a further increase to roughly 1200°C at 800 km depth and reaching temperatures of about 1400°C at 1100 km depth.

4. Previous Geophysical Constraints on Bulk Lunar Composition

[18] *Buck and Toksöz* [1980] conducted one of the first studies trying to constrain lunar bulk composition using geophysical data available at the time. These were upper and middle mantle seismic velocities, near-side crustal thickness and seismic velocities, center-of-figure to center-of-mass offset, mean density and moment of inertia. They tested a broad range of models against these geophysical constraints, by converting the chemical abundances suggested for the bulk Moon into mineralogical abundances for a layered Moon and then found the resulting seismic and density profiles. Specifically, only the major oxide components, FeO, MgO, SiO_2 and Al_2O_3, were modeled. Furthermore, as the system was deemed underdetermined, given the available constraints, Al_2O_3 was taken out and fixed at various values. The CaO was also fixed using the average value for the Ca/Al weight ratio of 1.10, as determined by *Ahrens and von Michaelis* [1969] from a number of meteorite classes. Assuming the crust to have an average thickness of 75 km and to consist of troctolite as average composition ($\rho \sim 3.0$ g/cm^3), they determined seismic velocities as a function of depth for a number of mineral assemblages and then compared these with the seismic velocity model of *Goins et al.* [1978]. Once the composition fit the adopted seismic velocity model it was tested against the constraints of mean density and moment of inertia. For this, the density profile was calculated using a single thermal profile [*Toksöz et al.*, 1978] and a second order Birch-Murnaghan equation of state to account for pressure. To make sure that models were within the uncertainties of the moment of inertia, cores with a density of ~6 g/cm^3, taken as being representative of the density of Fe-FeS at STP conditions, were added. Their study revealed that best fits to all constraints were obtained for those models that (1) included bulk compositions with less than 5 wt% Al_2O_3, (2) contained cores, ranging from 1 to 2 wt% of the bulk Moon and (3) had several wt% Fe-FeS in the middle mantle (below 480 km depth in their model) to be consistent with the seismic velocity drop in this region found in the Goins model.

[19] The main objection to be raised about this study, apart from the fact that *Buck and Toksöz* [1980] only consider one possible thermal profile, concerns the seismic velocity model adopted from *Goins et al.* [1978], which has also been pointed out by *Hood and Jones* [1987]. This model was derived in the late 1970s, just after termination of the Apollo lunar seismic experiment at a time when the entire data set had not yet been analyzed, and was subject to a more limited number of events, particularly the deep moonquakes. Contrary to later findings, velocity decreases were found to exist between the upper and middle mantle, notably in the depth range 400–480 km, which by the authors was taken as being the zone to which the early Moon had differentiated to produce the anorthositic crust. As also pointed out by Buck and Toksöz, their initial mantle compositions produced velocity increases and not decreases in the middle mantle due to the onset of the garnet stability field at this depth. In order to lower the velocities the authors suggested a number of possibilities, such as lowering the Mg#, i.e, increasing the Fe content of the silicates (leading to an increase in density, but a decrease in seismic velocity) or, the chosen alternative, to augment the content of free reduced iron and iron sulfide. Adding Fe-FeS in the middle mantle, thereby increasing its density, leads to a reduction of the core mass needed to satisfy the moment of inertia and an FeS core with a radius of ~340 km, representing 1 wt% of lunar mass, was found to be the preferred scenario. Also, models containing more than 5 wt% Al_2O_3 were rejected as the increased amount of Al produced even more garnet at this depth and resultingly higher velocities, in disagreement with the adopted seismic model.

[20] *Hood and Jones* [1987] conducted a study along the lines of *Buck and Toksöz* [1980], but wanting to place fewer constraints on their models, considered a series of proposed lunar bulk compositions, thermal and early differentiation and evolution models to calculate mantle seismic and density profiles. These were then compared to the constraints imposed by geophysical data, to assess, among other things, the resemblance of bulk lunar composition to the Earth's mantle and the need for a metallic core. As geophysical constraints, Hood and Jones considered mean density, moment of inertia, mean crustal density and thickness, and mantle seismic velocity limits as determined by *Nakamura* [1983].

[21] The complete analysis of the 8-year Apollo lunar seismic data set had been finalized in the early 1980s [*Nakamura et al.*, 1982; *Nakamura*, 1983] and the lunar seismic velocity model underwent a revision in comparison to the one published by *Goins et al.* [1978, 1981], notably in regard to mantle structure. The number of deep moonquakes used rose from 24 to 41, providing greater sensitivity in the middle mantle. The Nakamura model shows velocity increases at depths of around 500 km, rather than velocity decreases apparent in the Goins model.

[22] As noted, in order to provide more leniency in the modeling, *Hood and Jones* [1987] assumed four bulk composition models and coupled these with three different thermal models and four simple differentiation schemes. The thermal models were taken from *Schubert et al.* [1977], *Toksöz et al.* [1978] and *Binder and Lange* [1980], as representative samples of the present-day lunar thermal

Table 1. Literature Estimates of Bulk Composition Models in wt% of the Silicate Part of the Moon and Earth[a]

Model	CaO	FeO	MgO	Al_2O_3	SiO_2
	Moon				
Ringwood [1979]	3.7	14.1	32.9	4.2	45.1
Taylor [1982] bulk model	4.6	13.1	32.3	6.1	43.9
Wänke and Dreibus [1986]	3.8	13.1	32.6	4.6	45.9
O'Neill [1991]	3.3	12.4	35.1	3.9	44.6
Kuskov and Kronrod [1998] I	4.8	10.4	28.5	6.3	50.0
Kuskov and Kronrod [1998] II	4.3	11.7	29.6	5.9	48.5
Warren [2005]	3.0	9.1	35.6	3.8	46.2
Taylor [1982] crustal model	16.5	6.5	7.0	25.0	45.5
	Earth				
McDonough and Sun [1995]	3.6	8.2	38.2	4.5	45.5

[a]Note that only the contents of the CFMAS elements are given.

state calculated from thermal history models. As regards the four compositional models considered, these were taken from *Morgan et al.* [1978], *Taylor* [1982], *Wänke et al.* [1977] and *Delano* [1986] and were chosen because of their large range of Al_2O_3 (3.5 to 7.6 wt%) and FeO (10.9 to 16.3 wt%) concentrations, which as argued by the authors, are important, as Al is a main constituent of spinel and garnet. Being relatively dense phases with high seismic velocities, the abundance of these minerals can critically influence the interpretation of seismic velocity and moment of inertia constraints. The FeO content also plays an important role in controlling the seismic velocities and densities of mafic minerals, since these properties are sensitive to the Fe/(Fe + Mg) ratio of the mantle. All four differentiation schemes included a mean crustal thickness of 70 km and the crustal composition of *Taylor* [1982] (see Table 1), corresponding to a density range of between 2.9 and 3.05 g/cm^3 if slight uncertainties are taken into account. Beneath this crustal layer one model was entirely homogeneous, corresponding to whole-Moon differentiation, the second one assumed differentiation to 500 km and a pristine mantle beneath, the third one included differentiation to a depth *d* (defined as the minimum depth to which the Moon had to be differentiated in order to extract the necessary Al to form the crust) and a pristine composition underneath and finally, the fourth one considered differentiation to depth *d*, with a well-mixed interior beneath 500 km.

[23] By permuting the proposed thermal, bulk and differentiation models, 33 models were found to be realistic and were subsequently used to calculate seismic velocity and density profiles. Given the chemical composition, temperature and pressure as a function of depth, modal abundances of olivine, diopside and orthopyroxene ± (plagioclase, spinel, garnet, jadeite, Mg-tschermakite and Ca-tschermakite) were calculated within the three mineral stability fields of plagioclase, spinel and garnet, with the plagioclase-spinel and spinel-garnet transitions set at 200 km ($\sim$10 kbar) and 500 km ($\sim$23 kbar), respectively. Model assemblage velocities were determined from bulk modulus, shear modulus and bulk density, which themselves were determined from the elastic moduli of the component minerals along with their volume fractions, using Hashin-Shtrikman bounding. *Hood and Jones* [1987] found that most of their calculated velocity models fit the Nakamura model qualitatively. However, they favored those that assumed differentiation of the upper mantle only (<500 km depth), contained a greater bulk concentration of Al_2O_3 than the terrestrial mantle (>6 wt%) and were distinguished by an increase in Mg# beneath the upper and middle mantle, to account for the velocity increase at 500 km depth which characterizes the Nakamura model. The density models were found to be unable to satisfy the adopted moment of inertia value at the 1-σ limit and the authors concluded that a small dense core of 1–4 wt% was needed. While the study of *Hood and Jones* [1987] picks samples from the space of compositional, thermal and evolution models, and thus represents an improvement over the study by *Buck and Toksöz* [1980], only a limited number of models were investigated.

[24] In the study of *Mueller et al.* [1988] an inverse approach was adopted. The authors tried to obtain a range of compositional models consistent with the Nakamura model and petrological arguments. The chemical composition of the Moon was modeled within the CFMAS system and the major oxides were assumed to occur in the minerals olivine, orthopyroxene, diopside, anorthite, spinel or garnet (the latter three depending upon depth). The spinel stability field ranged from 180 to 500 km depth. The abundance of calcium was scaled to that of aluminum with a chondritic ratio. As regards the temperature distribution throughout the lunar interior, a linearly increasing and superadiabatic upper mantle thermal profile was adopted, implying a nonconvective region that essentially contains no radioactive elements. Velocities of mineral assemblages were determined in a manner equivalent to the one used by *Hood and Jones* [1987]. Results indicated that in order for the upper mantle seismic velocity model of Nakamura to be in agreement with the constraints imposed by mass and moment of inertia, a metallic core with a radius of at least 150 km was necessary. After addressing the question of whether bulk lunar composition bears any resemblance to that of the terrestrial mantle, Mueller et al. conclude that this is only possible in the extreme case, as they find a lunar Mg# that is too low and an abundance of Al that is too high in comparison to the Earth.

[25] In a series of papers, Kuskov and collaborators [e.g., *Kuskov*, 1997; *Kuskov and Kronrod*, 1998, 2001; *Kuskov et al.*, 2002] have undertaken thermodynamic modeling of the chemical composition of the Moon with ever increasing complexity, from initially within the CFMAS system to most recently within the NaTiCFMAS system. Here we will concentrate on the study of *Kuskov et al.* [2002]. The authors use a Monte Carlo scheme, i.e., a random number generator, to randomly vary the chemical composition, producing velocity and density profiles which are then compared to the adopted seismic velocity model, mass and moment of inertia.

[26] Geophysical constraints adopted by *Kuskov et al.* [2002] include the Nakamura seismic velocity model, as well as the latest determinations of lunar mass and moment of inertia by Lunar Prospector [*Konopliv et al.*, 1998]. The model follows earlier investigations by adopting the seismic discontinuities of the Nakamura model as delineations between crust, upper, middle and lower mantle. An average crustal thickness and density of 60 km and 3.0 g/cm^3 are chosen. As the authors correctly note, the bulk composition of the Moon is a priori unknown, leading them to consider a large range of input compositions. The major mantle oxide concentrations are allowed to vary in steps of 1 wt% within

the ranges, $2 \leq$ CaO, $Al_2O_3 \leq 7$ wt% (Kuskov et al. fix CaO to Al_2O_3 by assuming a Ca/Al ratio of 1.25), $25 \leq$ MgO ≤ 45 wt%, $40 \leq SiO_2 \leq 57$ wt% and $6 \leq$ FeO $\leq$ 20 wt%, representing ranges of these oxides in the Earth, Moon and silicate fraction of chondrites. The concentrations of Na_2O and TiO_2 are set equal to their chondritic content. Regarding the variation of temperature in the mantle, Kuskov et al. assumed a temperature profile of the form $T(^\circ C) = 430 + 1250(1 - \exp[-0.00125[H - 60]])$, where H is depth as measured from the base of the crust. To additionally test the robustness of their approach they allowed the temperature in the upper and middle mantle to vary by ±100°C and ±200°C, respectively. The computation of the mineral assemblage from the chemical composition was performed using a method of minimization of Gibbs free energy and thermodynamic data for minerals and solid solutions, while the subsequent determination of elastic moduli of the equilibrium mineral aggregates was subject to standard Voigt-Reuss-Hill averaging. The authors tested a broad range of models and found an equal spread of density and velocity profiles.

[27] The conclusions drawn by the authors were that cores, amounting to between 2 and 4 wt%, are needed in order to satisfy the moment of inertia. However, core-free models were also found to be a distinct possibility, but only if lower mantle (>500 km depth) densities lie in the range 3.49 to 3.52 g/cm^3. *Kuskov et al.* [2002] found bulk silicate Mg#s of 80–82. In addition, they also found that the bulk alumina content of the silicate portion of the Moon lies between 5.5 and 7.0 wt% and that "the Moon is depleted in MgO and enriched in refractory elements compared to the terrestrial mantle" and furthermore that it "bears no genetic relationship to the terrestrial mantle as well as to any of the known chondrites" [*Kuskov and Kronrod*, 1998, p. 302].

[28] Having summarized previous investigations, let us reemphasize to the reader why further analysis of the problem of constraining bulk lunar composition from geophysical data is warranted. First of all, none of the aforementioned studies are actual inversions of the Apollo lunar seismic data; previous workers adopt a seismic velocity model including its parameterization and associated uncertainties, which they try to fit with one or more chemical compositions and thermal models. The potential problems with such an approach, were also discussed by *Nakamura* [1983] and *Hood and Jones* [1987], who note that the derived velocity model only represents an approximation to the actual velocity structure, with the layer boundaries at 270 km and 500 km depth not necessarily being real. Second, given our underlying philosophy of assuming the bulk composition of the Moon essentially unknown, the restrictions imposed by previous authors are, by our standards, too restrictive. As we have seen, this not only concerns bulk composition, but also thermal state, as there is a very limited data set available to constrain the latter.

5. Geophysical Data and Uncertainties

[29] The geophysical data used here are lunar seismic arrival times from a number of diverse events, including 8 artificial impacts, 19 meteoroid impacts, 8 shallow moonquakes and 24 deep moonquakes, as registered at the four stations installed during the Apollo missions 12, 14, 15 and 16. The 59 events considered here resulted in a total of 318 first P- and S-wave arrivals which are used in the present inversion (the arrival time picks and associated uncertainties are tabulated by *Lognonné et al.* [2003]). The details concerning the experiment will not be elaborated here and the reader is referred to, for example, *Latham et al.* [1969], *Toksöz* [1974], *Toksöz et al.* [1974] and *Nakamura et al.* [1980, 1982] for further details. A couple of qualifying comments concerning the Apollo lunar seismic data set, however, are appropriate at this point.

[30] It is at present the only extraterrestrial seismic data set which can be used to infer the interior structure of a planetary body besides the Earth and because of this constitutes a unique and extremely valuable resource. However, it should not be forgotten that because of the scanty nature of the data set and especially its quality (lunar seismic signals are characterized by their anomalously long duration, their reverberating nature, slowly building amplitudes and long decay of the wave train, ensuring that anything arriving after the first arriving P and S waves is essentially obscured in the coda), a certain subjectivity is automatically introduced on the part of the investigator, as his or her judgment as to when a particular arrival is actually observed is a matter of personal taste. However, if the data set is large enough these inconsistencies will be smoothed out and the final results of the inversion are less prone to be biased. On the other hand, if the data set is not characterized by such a redundancy, objectivity cannot be attained and differences in data interpretation among different observers can significantly alter the models obtained and it is indeed the case that, whichever inverse method is used, the results obtained by different scientists from such data sets are different, as pointed out by *Tarantola* [1987].

[31] This situation is excellently exemplified by the Apollo lunar seismic data set. During the Apollo era, two data sets were under consideration, one by the MIT group [e.g., *Goins et al.*, 1981] and the other one by the Galveston group (University of Texas) [e.g., *Nakamura et al.*, 1982]. While differing not only in arrival time readings, they also differed, as already discussed, in the number of readings, notably in the number of deep moonquakes used, with *Goins et al.* [1981] considering only 24 events in comparison to 41 by *Nakamura* [1983]. Although they both used linearized techniques to invert the data, they obtained quite different inversion results and whence interpretations of the lunar internal structure. The Goins model was characterized by velocity decreases between the upper and middle mantle, whereas the Nakamura model showed the velocity to increase in this region (for the description here, our division of the Moon generally follows that of *Nakamura* [1983] where the Moon is divided into a crust, ~60 km thick, an upper mantle extending to ~500 km, a middle mantle continuing down to ~1100 km depth and possibly a lower mantle covering the depth range ~1100–1400 km with the core making up the rest, although it should be noted that for the discussion of our results we adopt a division of the mantle into an upper and lower, only). A positive velocity discontinuity marking the upper/middle mantle transition was also found in another recent analysis, where the Nakamura data set was reinvestigated using a nonlinear

Monte Carlo inversion technique [*Khan and Mosegaard*, 2002]. On the other hand, *Lognonné et al.* [2003], who reanalyzed the lunar seismic data set with particular attention to estimation of uncertainty on individual arrival time readings, which the authors claim to be the main reason why they undertook the endeavor of reanalyzing the data set, used only 24 deep moonquakes events in their inversion and found *P*- and *S*-wave velocity decreases at depths of ~500 km and ~700 km, respectively, leading them to state that discontinuities in the mantle are not well resolved. Lognonné et al. considered only 24 deep events because the uncertainty on the remaining events were deemed to be too large to result in any meaningful information.

[32] So, what is one to make of all these discrepant models and moreover is it possible to circumvent the bias? In the work of *Nakamura* [1983], arrival time readings from several different investigators have been compiled and a mere glance at the picked arrivals makes us recognize that we are indeed faced with a problem vis a vis the aforementioned data objectivity, since readings can differ by up to 20 s or more and the question of how to minimize bias is not easily answered. One might consider the possibility mentioned by *Nakamura* [1983], of averaging the arrivals read by up to four different analysts. However, from a probabilistic point of view this is not recommended as the averaging of travel time readings of two different investigators of, for example, 150 s and 165 s, with uncertainty readings of, say, 5 s each, will produce a mean of 157.5 s, which does not lie within either sphere considered by the analysts. As there is no simple solution to the problem of minimizing subjectivity, we have presently chosen to focus attention on the data set obtained by *Lognonné et al.* [2003]. A priori, there is no reason to believe any given data set more credible than any other, although it has to be noted that there are probably more reasons to consider the latest data set reevaluated by *Nakamura* [2005] as state of the art, as the number of deep moonquakes used by him totals almost 4000 events (this precludes the events from the newly identified nests) as compared to only 1360 back in the early 1980's.

[33] The other geophysical data used are lunar mass and moment of inertia, which hold the potential of not only constraining the density profile but also providing information on the lunar core. The values adopted are $M = 7.3459 \pm 0.001110^{22}$ kg and $I/MR^2 = 0.3935 \pm 0.0002$ [*Wieczorek et al.*, 2006], based on the moment of inertia value of 0.3931 obtained through the analysis of Lunar Prospector [*Konopliv et al.*, 1998] and rescaled to a mean radius of 1737.1 km [*Smith et al.*, 1997].

6. Method of Analysis

[34] The inverse problem treated here is written in general terms as

$$\mathbf{d} = g(\mathbf{m}) \tag{1}$$

implying the calculation of data **d** given a set of model parameters **m** (the forward problem) or conversely, inference of values of the model parameters from observed data (the inverse problem). **g** is a (usually nonlinear) functional relation governing the physical laws that relate model and data, expressing our mathematical model of the physical system under study. The solution to the general inverse problem within the Bayesian framework is given by [*Tarantola and Valette*, 1982; *Mosegaard and Tarantola*, 1995]

$$\sigma(\mathbf{m}) = k\eta(\mathbf{m})\mathcal{L}(\mathbf{m}), \tag{2}$$

where k is a normalization constant, $\eta(\mathbf{m})$ is prior information on model parameters and $\mathcal{L}(\mathbf{m})$ is the likelihood function and can be construed in probabilistic terms as a measure of how well a given model fits data. Before describing the model, prior information and the likelihood function, let us briefly mention how data are calculated from a knowledge of composition and temperature.

[35] This is most easily explained by breaking equation (1) up into a number of forward modeling sequences,

$$\begin{tikzcd} & & \mathbf{d}_2 \\ \mathbf{m} \arrow[r, "g_1"] & \mathbf{d}_1 \arrow[ur, "g_2"] \arrow[dr, "g_3"] & \\ & & \mathbf{d}_3 \end{tikzcd} ,$$

where **m** is an assumed starting composition and temperature profile, g_1 is the forward operator embodying the thermodynamic calculation of mineral phase proportions (modal mineralogy) and their physical properties, in the form of the density and seismic wave velocities, $\mathbf{d}_1$ is a data vector containing modal mineralogies, mineral densities and wave velocities, g_2 is the physical law calculating seismic arrival times given a seismic wave velocity model, $\mathbf{d}_2$ are calculated arrival times, g_3 is the operator that calculates mass and moment of inertia and finally, $\mathbf{d}_3$ is the data vector containing mass and moment of inertia.

[36] The lunar mineralogy is assumed to be dictated by equilibrium and is computed from thermodynamic data for a given model pressure, temperature and bulk composition by Gibbs energy minimization [*Connolly*, 2005]. Seismic velocities were computed as outlined by *Connolly and Kerrick* [2002] using the shear modulus data base summarized in that work and modified by data for olivine, clinopyroxene and orthopyroxene [*Vacher et al.*, 1998]. Bulk seismic velocities were computed using bulk elastic moduli obtained as the Voigt-Reuss-Hill volumetric average of the mineral moduli under the assumption that textural anisotropy is negligible [*Watt et al.*, 1976].

[37] Our spherically symmetric model of the Moon is divided into three layers: a crust, a mantle and a core. Thermodynamic modeling is restricted to the layers comprising crust and mantle, as metallic Fe is not included in the compositional space. Crust and mantle layers are variable in size, modeled by depth d and are assumed to be uniformly distributed within the following intervals $30 < d_{crust} < 60$ km, $d_{crust} < d_{mantle} < d_{CMB}$, where d_{CMB} is the depth to the core mantle boundary and the radius of the Moon is anchored at $r_{moon} = 1737$ km. The depth to the CMB is determined as $d_{CMB} = r_{moon} - r_{core}$, where r_{core} is the variable core radius. The core is parameterized in terms

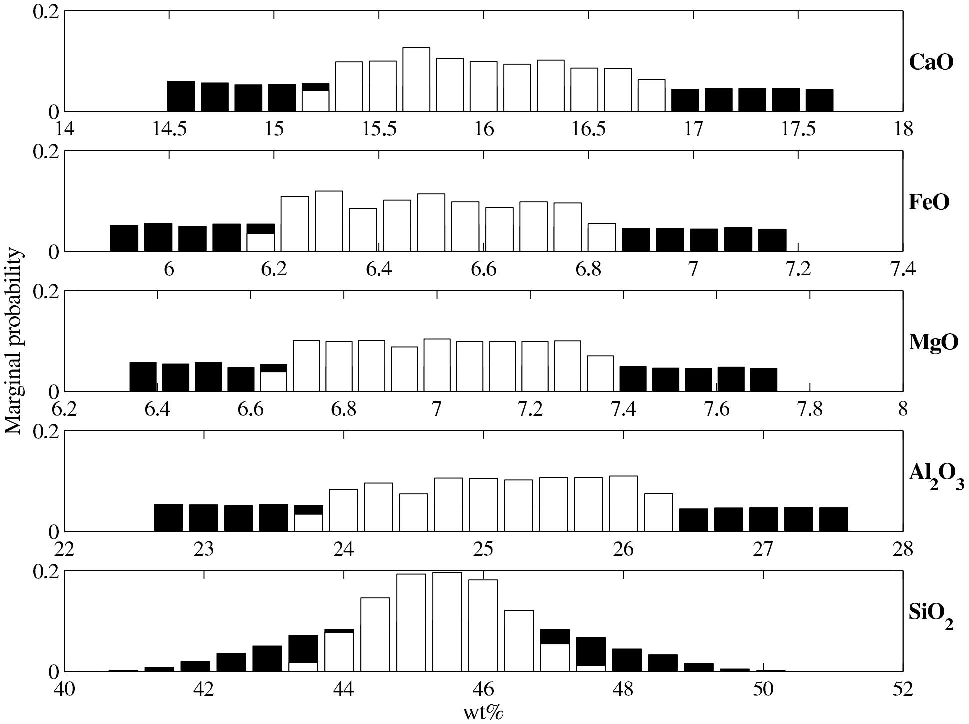

Figure 1. Prior (black) and posterior (white) marginal *pdf*'s for the oxide elements in the CFMAS system (marked to the right of each panel) making up the crustal composition. The relatively flat posterior distributions are evidence of the reduced sensitivity of the data to the crustal composition, which is the main reason why we chose a priori to bound the crustal composition to within 5% of the Taylor composition (see Table 1).

of its radius and density (ρ_{core}). These are distributed uniformly in the intervals $0 < r_{core} < 400$ km, $\rho_m < \rho_{core} < \rho_c$, where ρ_m is the value of ρ at the base of the mantle as estimated by VERTEX and $\rho_c = 7.5$ g/cm^3.

[38] Temperature T is parameterized at six fixed nodal points, corresponding to depths of 0, 200, 400, 500, 1000 and 1700 km. At each of these nodes the logarithm of T is uniformly distributed in the interval $T_k \in [T_{k-1}; T_{k+1}]$, with the added constraint that $\ldots, T_{k-1} \leq T_k \leq T_{k+1} \ldots$, to prevent temperatures models from decreasing as a function of depth. We have chosen the peridotite solidus of *Hirschmann* [2000] as an upper bound, here labeled T_p, so that in any given layer k there also exists the constraint $T_k < T^p_k$. Surface temperature is held constant at 0°C.

[39] Crust and mantle are additionally parameterized using the composition c, which designates the wt% of the elements CaO-FeO-MgO-Al_2O_3-SiO_2. These are log-uniformly distributed within certain intervals, corresponding to $1 < CaO < 8$ wt%, $5 < FeO < 15$ wt%, $20 < MgO < 55$ wt%, $1 < Al_2O_3 < 8$ wt% and $35 < SiO_2 < 55$ wt% and with the added constraint that in each of the two layers $\Sigma_i c_i = 100$ wt%. Moreover, the minor elements ratio Ca/Al $\in [0.5;2]$. For the crust we assumed the Taylor composition [*Taylor*, 1982] and varied the concentration of the five elements by 5 wt% around this model of the crust (see Table 1). Further technical details are given by *Khan et al.* [2006].

[40] Under the assumption that the observational uncertainties and calculation errors are independent among the different geophysical methods employed and additionally making the assumption that data uncertainties can be modeled using an l_1-norm, the likelihood function takes the following form:

$$\mathcal{L}(\mathbf{m}) \propto \exp\Bigg(-\frac{|d^I_{obs} - d^I_{cal}(\mathbf{m})|}{\sigma_I} - \frac{|d^M_{obs} - d^M_{cal}(\mathbf{m})|}{\sigma_M} - \sum_i \frac{|d^{P_i}_{obs} - d^{P_i}_{cal}(\mathbf{m})|}{\sigma_{P_i}} - \sum_j \frac{|d^{S_j}_{obs} - d^{S_j}_{cal}(\mathbf{m})|}{\sigma_{S_j}} \Bigg), \qquad (3)$$

where d_{obs} denotes observed data, $d_{cal}(\mathbf{m})$ synthetic data computed using model $\mathbf{m}$ with superscripts alluding to the particular geophysical observation and σ is the uncertainty on either of these. In all, we sampled 1.2 million models from which 12,000 were kept for analysis here, which all fit data to within uncertainties.

7. Results and Discussion

7.1. Crust

[41] The crust, in this study, is not accorded the same importance as the mantle, given that data for the most part sense the mantle to a much larger extent. This is reflected in the much higher number of seismic rays traversing the mantle compared to the crust and is the main reason why we chose to bound the crustal composition around the model of *Taylor* [1982]. Figure 1 shows the crustal composition in the form of one-dimensional (1D) prior and posterior marginals for the oxides in the CFMAS system. The reduced data sensitivity to crustal composition is obvious when contemplating the probability distributions.

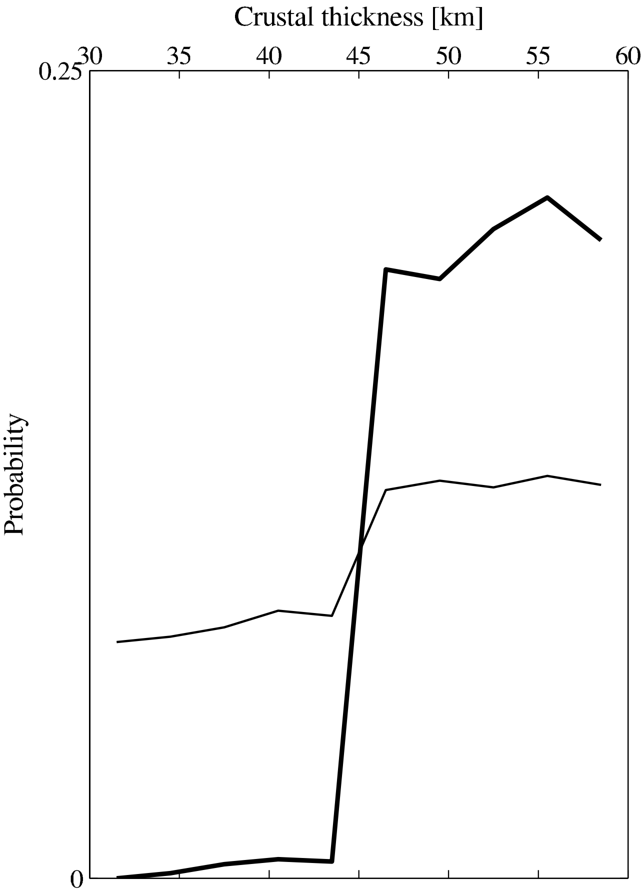

Figure 2. Prior (thin line) and posterior (thick line) *pdf*s, depicting sampled crustal thickness values.

Almost homogeneous probability density functions (*pdf*s), centered on the Taylor model, are obtained. The compositions imply Mg#s of around 66 in general agreement with observations from sample analysis [*Warren*, 1986; *Ryder and Spudis*, 1987].

[42] The geophysical data indicate a crustal thickness in the Mare Cognitum region (in the vicinity of the Apollo 12 and 14 landing sites) of about 40–45 km [*Khan et al.*, 2000], in agreement with what has been obtained here (see Figure 2). The other recent crustal thickness estimate of 30 km [*Lognonné et al.*, 2003] is, as remarked by *Wieczorek* [2003], only "marginally consistent" with overall geophysical constraints.

[43] A low-density crust is generally implied by the overall density and moment of inertia constraints. Anorthositic gabbro containing ~25 wt% Al_2O_3, with a density of about 2.95 g/cm^3 is thought to be representative of the lunar highland crust [*Taylor*, 1982]. Early interpretation of the crustal seismic velocity profile [*Toksöz et al.*, 1974] suggested a division of the crust, with the uppermost 20 km characterized by somewhat reduced velocities due to the presence of porosity, which below this depth is thought to be completely annealed owing to conditions of increased pressure and temperature. Accordingly crustal density values as low as 2.7 g/cm^3 have been considered [e.g., *Bills and Ferrari*, 1977].

[44] Empirically determined elemental abundance correlations can be used to determine FeO/MgO and MgO/SiO_2 ratios, from which a representative lunar surface Mg# is derivable. *Warren* [1986] advocates a Mg# of 68 for the uppermost lunar crust based on various soil compositions and lunar meteorites. Lower crustal components represented by the low-K Fra Mauro basalts indicate an Mg# of 70 ± 3 [*Ryder and Spudis*, 1987]. While these values do not directly indicate a varying crustal composition as a function of depth, there is evidence for the latter, as ejecta from basin forming impacts is observed to be more noritic [*Spudis et al.*, 1984; *Davis and Spudis*, 1985].

[45] There is widespread belief that this low-density crust originated by crystallization and subsequent flotation in a magma ocean [e.g., *Warren*, 1985]. The presence of this thick highland crust of plagioclase feldspar requires a Moon with a substantial refractory element content [*Taylor*, 1982]. This constraint is of course critically dependent upon both the thickness of the crust and its abundance of anorthosite. A recent estimate by *Wieczorek and Zuber* [2001] gives 29–32, 24–29 and 18–25 wt% Al_2O_3 for the upper, lower and most mafic lower crust. These authors also note that "an assemblage of plagioclase and mafic silicates would float if this assemblage was made of more than ~69% plagioclase by volume." The upper crust, on the basis of data from central peaks of complex craters, extends at least to a depth of 30 km. Assuming that the upper and lower crusts are equal in volume, this leads to an average crustal Al_2O_3 content of 28.5 wt% [*Wieczorek and Zuber*, 2001] compared to the earlier estimate of 24.6 wt% [*Taylor*, 1982].

7.2. Mantle

7.2.1. Magma Ocean Models and Mantle Seismic Discontinuities

[46] When discussing the lunar mantle, several key issues come to mind of which the most prominent include the presence of a mantle seismic velocity discontinuity and whether this discontinuity bears any relation to magma ocean models and early lunar differentiation. In magma ocean evolution models [e.g., *Taylor and Jakes*, 1974; *Kesson and Ringwood*, 1976; *Longhi*, 1977; *Snyder et al.*, 1992; *Hess and Parmentier*, 1995] the first phase to crystallize will be olivine, rich in magnesium (high Mg#), with later crystallizing cumulates becoming ever more iron rich (lower Mg#). After crystallization has proceeded about 3/4 of the way, plagioclase is expected to become a liquidus phase, which, owing to its low density will float. After about 90–95% of magma ocean crystallization, FeO and ilmenite-rich phases will start to solidify. These will sink and pile up on the already emplaced, but less dense, MgO-rich cumulate layer. Depending on the thickness of this overlying layer, a gravitationally unstable situation might ensue. In the gravitational overturn models of *Kesson and Ringwood* [1976] and *Hess and Parmentier* [1995] this unstable layering will result in the sinking of FeO-rich and ilmenite-bearing cumulates, which, as they are some of the last to solidify, will bring with them incompatible radioactive elements. The sinking and upwelling processes will result in stirring and mixing.

[47] The question of the depth of the magma ocean has been much debated, with values ranging from as low as 200 km [*Solomon and Chaiken*, 1976], based on the absence of any visible tectonic features on the lunar surface, to whole-Moon involvement. Geochemical estimates demand a min-

imum of 40% by volume, which equals a depth of ~500 km, but are consistent with a scenario of a totally molten Moon, as minimum amounts of Al_2O_3 have to be retained in the interior [*Taylor*, 1982]. At present, there is no general consensus as to its depth and whole-Moon melting is favored by some [e.g., *Taylor*, 1986], as it provides a straightforward mechanism for core formation, although it should be noted that a totally molten Moon is not a prerequisite for the latter [*Stevenson*, 1990]. If the magma ocean did not extend to the center of the Moon and if material beneath it escaped melting and differentiation, one might expect a boundary in either composition or phase. This boundary at the base of the magma ocean should in principle be visible via seismology.

[48] Indeed, a seismic discontinuity, separating the upper from the lower mantle, has featured prominently in most seismic velocity models obtained during the Apollo era, although there has been less agreement upon its depth, size and sign, i.e., whether positive or negative. As already mentioned, *Goins et al.* [1981] and recently *Lognonné et al.* [2003] obtained a velocity decrease (note that the depth of the discontinuity differs in the respective studies), whereas *Nakamura et al.* [1982] and *Khan et al.* [2000] found a positive velocity jump (at 500 km and 560 km depth, respectively).

[49] The nature of this discontinuity has been much debated and several models have been invoked in order to explain it, involving a change of phase and/or composition. The spinel to garnet phase transition has been advocated as a possibility [*Hood and Jones*, 1987; *Mueller et al.*, 1988], although it was generally believed inadequate as it could not account for the desired increase in density, (Hood and Jones do remark that garnet-rich assemblages are in near-agreement with the Nakamura seismic velocity model). As an alternative explanation for the discontinuity, *Nakamura* [1983] and *Hood* [1986] proposed a compositional change in terms of a transition to more MgO-rich mafic silicates (as magma ocean cumulates). Mueller et al., however, argue that an increase in Mg# alone could possibly lead to buoyant instability and favor a compositional discontinuity as representing a transition between a highly fractionated upper mantle and a relatively unfractionated/primordial lower mantle. In the case of a pristine lower mantle, it is assumed that only the upper part of the Moon experienced melting and subsequent differentiation. With regard to this scenario, the investigations carried out by *Hood and Jones* [1987] and *Mueller et al.* [1988] have tried to link the 500-km seismic discontinuity of the Nakamura model to the magma ocean. These workers assume that the seismic discontinuity represents the base of the magma ocean, separating a differentiated upper mantle from an undifferentiated, pristine lower mantle. They find that models where differentiation of the upper mantle only is assumed, and are characterized by a greater bulk Al_2O_3 content as well as containing steep upper mantle and less steep lower mantle thermal gradients, are those that best explain the large velocity increase, because of the presence of high velocity garnet-bearing assemblages.

[50] A different explanation has also been offered by *Wieczorek and Philipps* [2000], who interpreted the mantle seismic discontinuity as representing the maximum depth of melting of the mare source region. In wanting to investigate the thermal evolution of the Moon within a setting where the heat-producing elements are concentrated in the Procellarum KREEP terrane, encompassing Oceanus Procellarum and Mare Imbrium which are known to contain high abundances of KREEP [e.g., *Haskin*, 1998; *Jolliff et al.*, 2000; *Korotev*, 2000], Wieczorek and Philipps showed that melting of the mantle was confined to the region beneath the terrane and that the mantle melted to no more than 600 km depth. There is evidence that the picritic glasses (see next section) originated from depths <500 km, which led Wieczorerk and Philipps to postulate that the upper/lower mantle seismic discontinuity represents the maximum depth of melting from which the mare basalts were extracted. Moreover, the upper mantle in this model is predicted to be depleted in Al_2O_3, while the mantle below the seismic discontinuity is expected to be relatively enriched in aluminous phases.

[51] In Figure 3 we have displayed the sampled seismic *P* and *S*-wave, as well as density profiles obtained here and major velocity changes in the mantle are not immediately apparent, which is related to the fact that we modeled the lunar mantle using a single composition. Any transitions between upper and lower mantle arising from a change in composition are thus obviously discounted, leaving only phase changes as a possible marker. We searched the entire set of sampled v_P and v_S models for any velocity changes in the mantle by correlating v_P and v_S at depths of 400 km and 750 km, respectively. No major velocity changes were found, reflecting the apparently remarkable homogeneity of v_P and v_S. A slight increase in v_P is discernible though, due to the coupled effects of pressure and slightly greater amounts of the higher velocity phase garnet. This is also reflected in the density profiles. The v_S is seen to decrease on going down through the mantle which is related to it being relatively more sensitive to temperature than v_P. Sampled temperature profiles are displayed in Figure 4. An almost uniform mantle is suggestive of extensive stirring and homogenization by convection as part of early lunar evolution, possibly during the period when the magma ocean was present.

[52] However, it has to be remarked that our results do not effectively rule out a possible discontinuity separating the upper from the lower mantle. As noted in section 1, one of the questions that we wanted to answer is whether the geophysical data are compatible with a single mantle layer or whether more complex scenarios are called for. While we are indeed able to fit data with our model, implying compatibility with a homogeneous mantle, and thus answering our question in the affirmative, more complex models of the lunar mantle cannot rigorously be excluded, as Occam's razor is at best a rule, not a law. The reality of a seismic discontinuity in the mantle will have to be left to future studies using expanded, and, hopefully, new data sets.

[53] The case for a lower mantle (>500 km depth) of primitive composition has also been made on the basis of the compositionally distinct source regions of the mare basalts in comparison to the volcanic glasses. Volatile-element contents and isotope ratios have established that the mare basalts and the volcanic glasses are derived from separate sources [e.g., *Tatsumoto et al.*, 1987]. In particular, results of recent studies of the trace element composition of mare basalts and picrite glasses have shown that for those

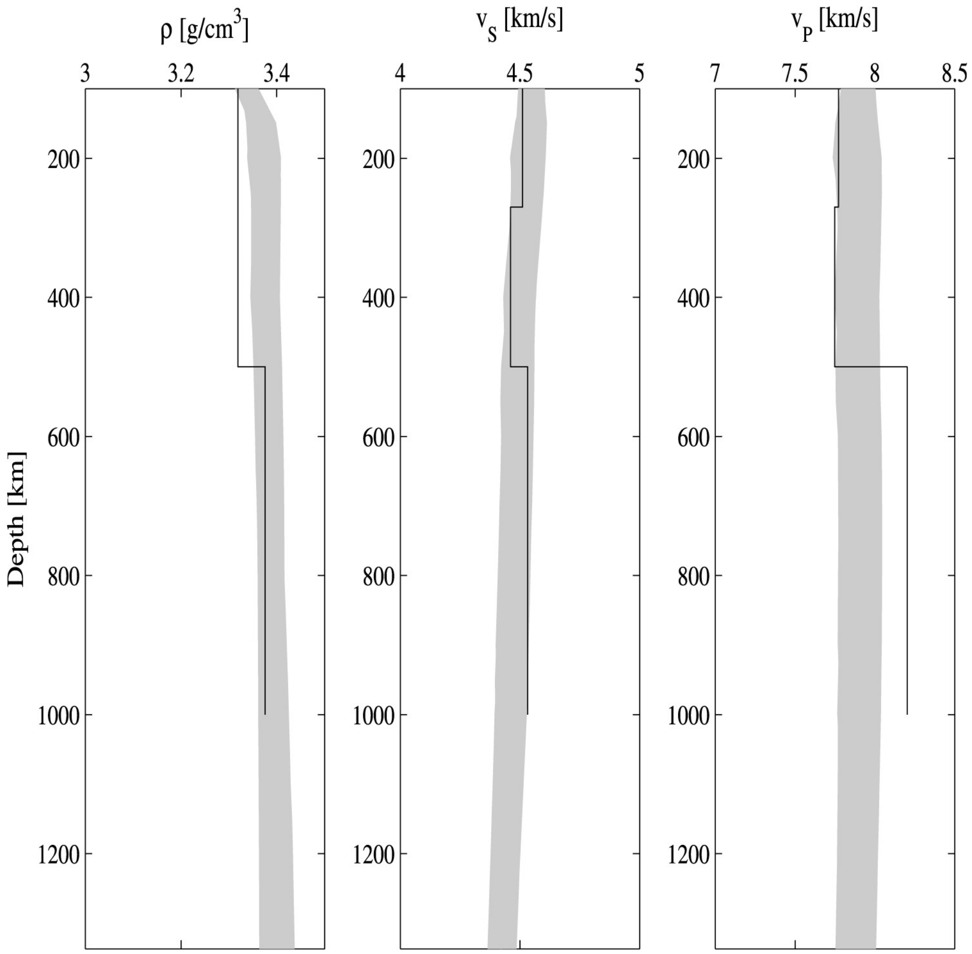

Figure 3. Models from the posterior distribution depicting (left) mantle density and (middle) *S*-wave and (right) *P*-wave velocity structure as a function of depth. In the figures, all sampled models have been plotted, with model II of *Kuskov and Kronrod* [1998] overlain for comparison.

samples with low Ti and little evidence of KREEP assimilation there remains a large variation in trace element ratios such as Sm/Yb [*Shearer and Papike*, 1993; *Neal*, 2001]. The factor of 3 variation observed in the Sm/Yb ratio of picritic glasses can be accounted for if garnet is present during melting in the lunar mantle. This led *Neal* [2001] to suggest that picrites with high Sm/Yb had been generated by melting in a deep, primitive part of the Moon which had not been part of a lunar magma ocean, while those with low Sm/Yb were derived from magma ocean cumulates. However, it is also possible that the range in Sm/Yb could be generated by varying degrees of melting of an initially garnet-bearing mantle, with high Sm/Yb produced at the early stages of melting and lower, near-chondritic Sm/Yb produced at high extents of melting once garnet had been exhausted from the residue. The presence of garnet during the generation of low Ti mare basalts has also been proposed on the basis of Lu-Hf ratios and Hf isotope systematics by *Beard et al.* [1998]. These observations are therefore consistent with our results showing the presence of 5–10 vol% garnet at depths of 200 km and deeper in the mantle.

[54] On the basis of the modeling results of *Kuskov and Kronrod* [1998], which showed that garnet was only a stable phase in the lower mantle (>500 km depth), *Neal* [2001] suggested that these particular glass beads were derived from the lower mantle. In addition, given the higher siderophile and chalcophile element abundances of these volcanic glasses relative to the mare basalts led Neal to further suggest that these were derived from a region of the Moon of primordial composition and therefore that the magma ocean did not encompass the entire sphere, although as also acknowledged by Neal himself, the data set upon which this is based is not very extensive. However, our alternative explanation for Neal's observation of the variation in the Sm/Yb ratio is in accord with a model without a midmantle discontinuity and can, with the present data, not be rigorously excluded.

7.2.2. Mantle Models and the Composition of the Lunar Basalts and Picrites

[55] Unlike for the crust, we do not possess any direct samples of the upper mantle and this region of the lunar interior can therefore only be characterized indirectly, either by studying geophysical data or through analysis of mare basalts that were produced by partial melting at depth and subsequently migrated to the lunar surface. The goal of a number of experimental studies has been to determine the pressures, temperatures and phases present when mare

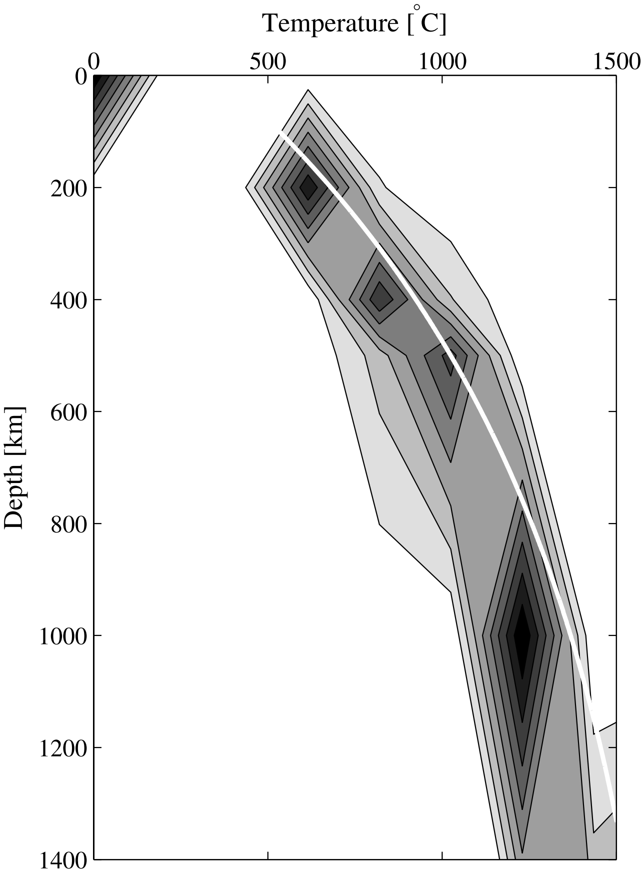

Figure 4. Marginal posterior *pdf*s depicting sampled temperature models as a function of depth. At six fixed depth nodes a histogram reflecting the marginal probability distribution of sampled temperatures has been set up. By lining up these marginals, temperature as a function of depth can be envisioned as contours directly relating its probability of occurrence. Shades of gray between white and black indicate, respectively, least and most probable outcomes. For comparison we have also displayed the thermal profile (model II) used by *Kuskov and Kronrod* [1998].

basalt and picrite glass compositions are in equilibrium with two or more solid phases at their liquidus. In the ideal case, when the erupted liquids are primary products of an isobaric batch melting process, such multiple saturation points are faithful indicators of the melting conditions within the moon. In a summary of experimental studies, *Longhi* [1992a] showed that primitive mare basalt compositions were multiply saturated with olivine and low-Ca pyroxene (either orthopyroxene or pigeonite) at pressures ranging between 0.5 and 1.25 GPa and that picrite glasses are saturated in these phases at higher pressure of 1.8–2.5 GPa. A simple interpretation of such results is that the lunar mantle should contain olivine and a low-Ca pyroxene at depths of between 50 and 500 km, and it is encouraging to note that olivine and orthopyroxene in our results (see Figure 5) constitute between 80 and 90% of the mass of the mantle over this depth range.

[56] However, given modern understanding of melt generation and transport processes in the Earth [e.g., *Kelemen et al.*, 1997], it is extremely unlikely that mare basalts and picrite glasses represent unmodified isobaric batch melts, and are probably more the products of polybaric fractional melting, with much of the transport of melt to the lunar surface taking place in high-porosity channels where reaction between melt and the host rock may occur. If melting is a polybaric fractional process in the Moon, then the significance of the multiple saturation pressures and mineralogies are less clear than for the isobaric batch melting case [*Longhi*, 1992b]. Detailed comparison of batch and fractional melting models has shown that the multiple saturation pressures in batch melting experiments are similar to the weighted average pressure of melt generation along a polybaric fractional melting path [*Asimow and Longhi*, 2004]. Therefore the experimentally observed multiple saturation of the mare basalts and picritic glasses in olivine and low-Ca pyroxene provides some support for the lunar mantle models shown in Figure 6, in that melts of these model compositions will be in equilibrium with olivine and orthopyroxene over a wide range of pressure conditions and over the bulk of their melting interval.

[57] While there is apparent consistency between our favored mantle compositional models and the melting experiments on lunar mare basalts and picrite glasses summarized by *Longhi* [1992a] in terms of olivine and low-Ca pyroxene saturation, up to 20% of the mass of the mantle in our models consists of high-Ca pyroxene and an aluminous phase (plagioclase, spinel or garnet). It is therefore interesting to note that only one of 15 low Ti samples tabulated by *Longhi* [1992a] shows liquidus saturation with augite, and only four show saturation with an aluminous phase. If our compositional models are correct, then two possible explanations for the rarity of clinopyroxene and aluminous phases on the experimental multiple saturation points can be advocated. First, if the extent of melting of peridotitic mantle exceeds 20 to 30% for typical pyrolite, then clinopyroxene and the aluminous phase will be exhausted from the solid residue. Therefore any further melting will produce liquids that are in equilibrium only with olivine and orthopyroxene, and the saturation temperature for clinpyroxene and the aluminous phase will drop to temperatures lower than that of the liquidus of the integrated melt from the entire melting interval. A different explanation follows on from a set of recent experimental work on picritic glass compositions [*Elkins-Tanton et al.*, 2003; *Draper et al.*, 2004; *Beck et al.*, 2006]. Although Elkins-Tanton et al. found only olivine and pyroxene on the liquidus of a synthetic analogue of Apollo 15A green glass at a pressure of 2.2 GPa and temperature of 1520°C, garnet is stable at temperatures ~20°C beneath the liquidus. Following the reasoning of *Asimow and Longhi* [2004], it is possible that such an arrangement of stable phases could have arisen from polybaric fractional melting over an interval which brackets 2.2 GPa. A multiple-saturation point involving liquid, garnet and a super-solvus high-temperature pyroxene has been proposed by *Draper et al.* [2004] for Apollo 15C green glass compositions at pressures of 2–3 GPa. This super-solvus pyroxene will break down to high- and low-Ca pyroxenes at subsolidus temperatures of under 1000°C, such as those preferred for our models. When melts that have been derived from deep olivine bearing sources rise and crystallize or react with their surroundings at low

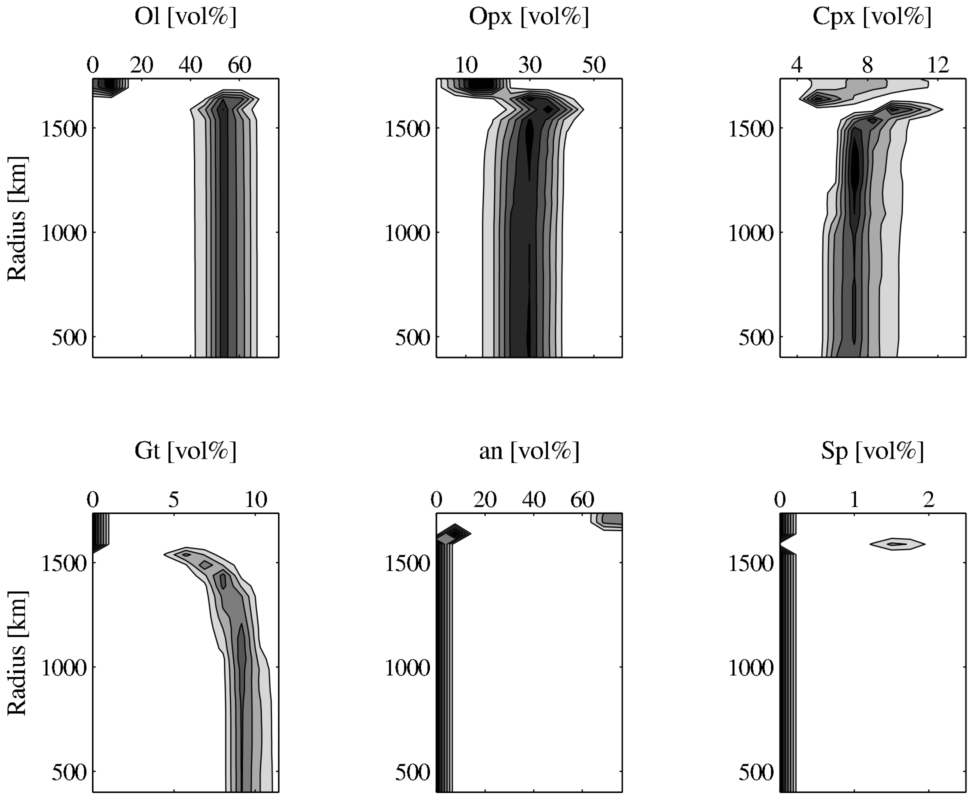

Figure 5. Marginal posterior *pdf*s of major minerals, showing the vol% of each phase as a function of radius. As in the case of temperature, at 31 fixed depth nodes a histogram reflecting the marginal probability distribution of sampled mineral proportions has been set up. By lining up these marginals, the mineral proportions as a function of depth can be envisioned as contours directly relating their probability of occurrence. Shades of gray are as in Figure 4.

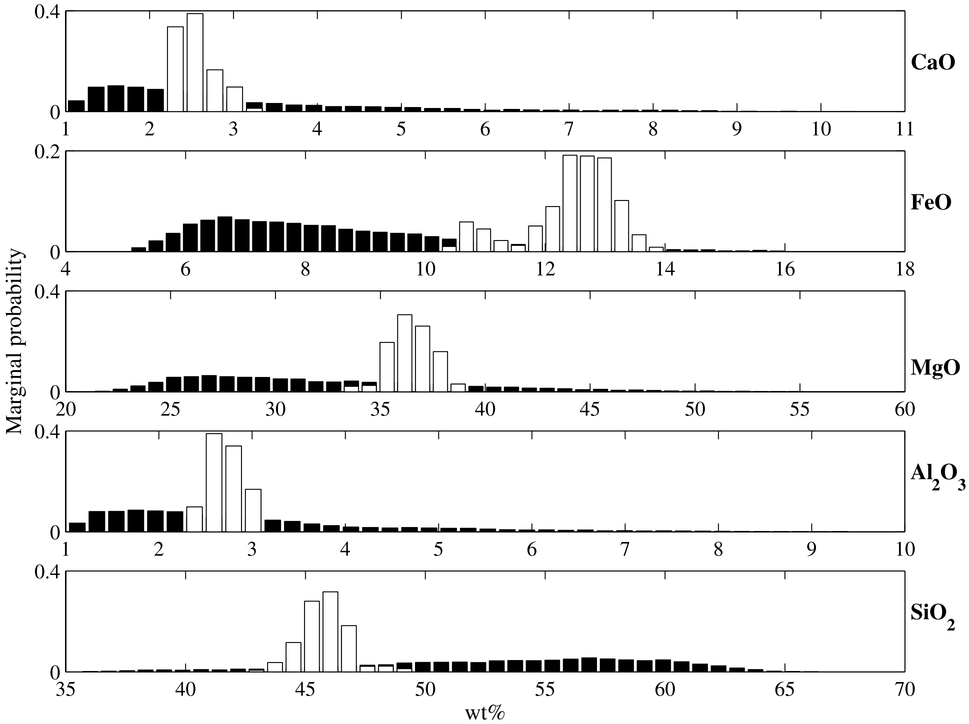

Figure 6. Sampled prior (black) and posterior (white) marginal *pdf*s for the oxide elements in the CFMAS system (marked to the right of each panel) making up the mantle composition.

pressure they will loose an olivine component. The experimental work of Beck et al. has shown that lunar picrite glasses can react rapidly with harzburgite in order to form dunite. The compositions of such evolving melts will therefore move away from the high-pressure olivine saturated liquidus composition. Therefore our preferred model mantle compositions may be related to green glass compositions by melting over a pressure range bracketing 2–3 GPa, followed by lower pressure olivine fractionation. The key point in this discussion is that the experimental work on the low Ti lunar mare basalt and picrite glasses cannot be used to discount the preferred lunar mantle composition recovered from the inversion of the geophysical data presented here.

7.2.3. Mg# of Picritic Glasses, Mg-Suite Cumulates, and the Mantle

[58] The estimation of the bulk Mg# of the lunar mantle from the compositions of the picritic glasses is fraught with difficulty, as described by *Warren* [2005]. The most primitive lunar glasses are in equilibrium with mantle sources with Mg#s of 77–84 mol [*Warren*, 2005], in broad agreement with the range of bulk mantle Mg#s of the accepted models shown in Figure 6. Therefore there are no obvious contradictions between the picrite glass compositions and the model mantle compositions proposed herein. However, the Mg# of the melt will be influenced not only by the mantle source composition, but also by the extent of the melting and any post-melting reaction and crystallization of mafic phases. Highly forsteritic olivines (Fo_{92}) reported from Mg-suite troctolites [*Hess*, 1994] cannot have been in equilibrium with small degree melts of the model mantle compositions shown in Figure 6, and must either have crystallized from liquids formed after large extents of fractional melting (over 25%) or derived from a heterogeneous mantle containing regions with high Mg#s. A number of authors have suggested that such regions may have developed in the early stages of crystallization of a lunar magma ocean [e.g., *Hess*, 1994].

7.2.4. Models of Mantle Melting

[59] In order to further understand the relationship between the mantle compositions recovered by the inversion of geophysical data and the compositions of mare basalts and picrite glasses a number of melting models were performed using the pMELTS algorithm [*Ghiorso et al.*, 2002] via the front end adiabat_1ph [*Smith and Asimow*, 2005]. The pMELTS algorithm is an updated version of the MELTS algorithm [*Ghiorso and Sack*, 1995], which uses thermodynamic models of minerals and melts to predict equilibrium phase assemblages and compositions and has been calibrated for melting of peridotite compositions at pressures of less than 3 GPa. The merits of pMELTS and adiabat_1ph have been discussed in detail by *Ghiorso et al.* [2002], *Asimow and Longhi* [2004] and *Smith and Asimow* [2005]. One problem with pMELTS is that there is a systematic error in the relationship between temperature and melt fraction, so that in order to attain a given melt fraction, model temperatures are 60°C higher than those observed experimentally. In the following discussion, therefore, we concentrate on the relationships between melt fraction and the major element composition of the melt and the modal mineralogy of the residual mantle, which are well reproduced by pMELTS. The largest errors in the oxide contents of the melt occur for MgO, which results in predicted Mg#s that are 2–3 mol% too high for a given extent of melting. This problem is most likely related to the temperature offset in the models [*Asimow and Longhi*, 2004]. The pMELTS algorithm also overstabilizes clinopyroxene, generating 5–10% more clinopyroxene at a given temperature than observed in peridotite melting experiments [*Ghiorso et al.*, 2002]. One advantage of using the adiabat_1ph front end is that trace element concentration variations in the melts and mineral phases can be calculated if a source composition and partition coefficients are supplied [*Smith and Asimow*, 2005]. We used the standard nonvariable partition coefficients supplied by these authors.

[60] A number of isobaric melting models were run at pressures of 0.5, 1.0 and 2.5 GPa, corresponding to depths where plagioclase, spinel and garnet, respectively, were found to be present in the model mantle compositions (Figure 6). Both equilibrium and fractional melting runs were performed, and a range of accepted mantle compositions from our inversions were used. The oxygen fugacity in the runs was fixed at the iron-wustite buffer, which is close to the fugacity expected for the lunar interior [*Longhi*, 1992b].

[61] The results of a garnet-field fractional melting model are shown in Figure 7. The model mantle composition was chosen from our ensemble of accepted mantle compositions shown in Figure 6 and lies close to the median of these models. The range of accumulated fractional melts generated from this model show a number of features in common with low Ti mare basalts and picritic glasses. Both mare basalts and picrite glasses have low CaO and Al_2O_3 contents, with low and very low Ti mare basalts from Apollo 12, 15 and 17 containing 7.3–11.2 wt% Al_2O_3 and 8.3–10.2 wt% CaO and Apollo 12 and 15 picrite glasses containing 7.1–7.9 wt% Al_2O_3 and 7.9–8.5 wt% CaO. Model melts with similar CaO and Al_2O_3 to the green glasses are produced after 20–30% melting at all the pressures studied. CaO and Al_2O_3 similar to that of the mare basalts is generated at <20% melting in the garnet field, but it is likely that these basalts have had their compositions modified by crystallization of mafic phases. In fact, the Mg#s of the Apollo 12, 15 and 17 low and very low Ti basalts (50–58 mol%) are not reproduced by melting of the mantle composition used in Figure 7, which has a Mg# of 84 mol%. The green glasses have Mg#s between 61 and 67 mol%, and these are reproduced during the first 20% of melting in Figure 7. Bearing in mind the systematic overestimation of liquid Mg# by pMELTS, and the likelihood that the picrite glasses have undergone limited to modest degree of crystallization or reaction in the shallow mantle, it is possible that melts parental to the green glasses could have been generated at more than 20% melting. In order to generate melts that are in equilibrium with the Fo_{92} olivines found in the magnesian suite troctolites [*Hess*, 1994], over 40% melting is required in the batch and accumulated fractional models. Instantaneous (not accumulated) fractional melts are in equilibrium with Fo_{92} olivines once more than 25% melting has taken place.

[62] The stability of the solid phases shown in Figure 7c shows that only olivine and orthopyroxene would be expected on the 2.5 GPa liquidus of mantle melts once the extent of melting exceeds 25%. Clinopyroxene is only

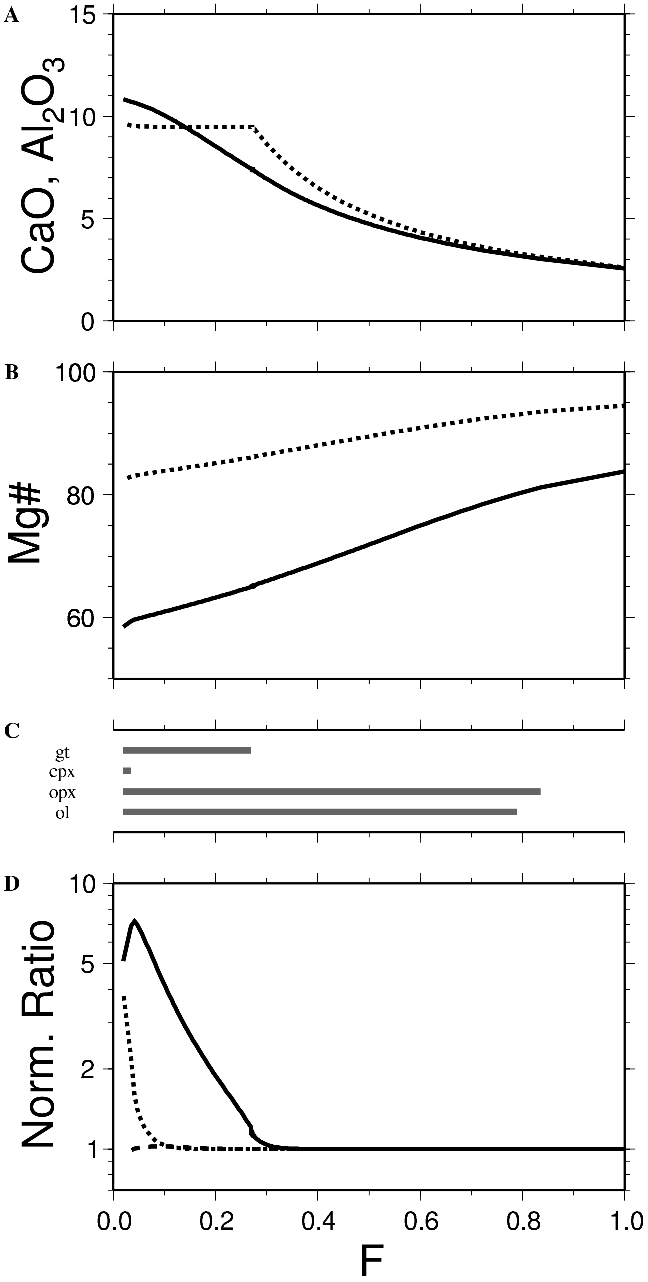

Figure 7. Results of model fractional melting at 2.5 GPa using a typical mantle composition of 2.29 wt% CaO, 11.09 wt% FeO, 31.97 wt% MgO, 2.33 wt% Al_2O_3, 41.65 wt% SiO_2. The *x* axis in all of the plots is the mass fraction of mantle melting, F. (a) CaO (solid line) and Al_2O_3 (dashed line) of the accumulated fractional melts. (b) Mg# of accumulated fractional melts (solid line) and equilibrium olivine (dashed line) calculated assuming a K_d^{Fe-Mg} of 0.3. (c) Stability range of solid phases in the melting residue. (d) Evolution of trace element ratios of accumulated fractional melts, normalized to their mantle source with $(Sm/Yb)_n$ as a solid line, $(La/Sm)_n$ as a short-dashed line, and $(Eu/Eu^*)_n$ as a long-dashed line. Eu^*_n is defined as $(Sm_n + Gd_n)/2$. The subscript *n* refers to concentrations normalized to mantle source. Note the log scale on the *y* axis.

stable for the first few percent of melting, and it is possible, given the overstabilization of clinopyroxene by pMELTS, that clinopyroxene would not feature on the 2.5 GPa liquidus of any melts of our model mantle composition. These results therefore reinforce the possible relationship between green glass compositions and our model mantle compositions as detailed in section 7.2.2 above.

[63] The evolution of trace element ratios shown in Figure 7d shows that large variation in the Sm/Yb ratio can be generated by variable extents of melting in the garnet field. This observation reinforces our earlier point that the layered mantle composition envisioned by *Neal* [2001], with pristine garnet-bearing lunar mantle sitting beneath olivine and orthopyroxene rich magma ocean cumulates, is not required by the trace element data. Variable extents of melting of a compositionally homogeneous garnet-bearing mantle, like that favored by the geophysical modeling, can also generate this variability.

7.2.5. Does Bulk Lunar Composition Resemble That of the Terrestrial Upper Mantle?

[64] Several lunar Mg#s ranging from 75 to 84 on the basis of petrological estimates have been proposed [*Ringwood*, 1979; *Taylor*, 1982; *Delano*, 1986]. This is generally lower than the Mg# of the Earth's upper mantle which, as also noted earlier, has been reasonably well estimated at 89 [*Ringwood*, 1979; *Palme and Nickel*, 1985]. The general observation that lunar basalts are more FeO-rich than terrestrial basalts [*Wänke and Dreibus*, 1986] has also been taken as an indication for a lower lunar Mg#. The geophysical models of *Kuskov and Kronrod* [1998] suggested bulk lunar Mg#s of about 82. A perusal of the literature, therefore, seems to suggest a Mg# ~10 mol% lower than the Earth's upper mantle, by and large in agreement with our findings of a significantly lower Mg# (~83). *Warren* [2005], on the other hand, using recent data from lunar meteorites, recalibration of the global Th data, based on the Lunar Prospector gamma-ray data [*Prettyman et al.*, 2002] and assuming chondritic proportionality among major elements, estimates a bulk Earth-like lunar Mg# of 87–88. Our sampled bulk silicate compositions and Mg# are summarized in Figure 8.

[65] The presence of garnet in the lower mantle implies the presence of Al_2O_3 and several attempts have been made at estimating the aluminum content of the Moon using various assumptions. *Taylor* [1982] has estimated the bulk Al_2O_3 content of the Moon, employing an average crustal Al_2O_3 content of 24.6 wt% and assuming a crustal thickness of 61 km (10% of lunar volume), as well as whole-Moon melting and a reasonable assumption of the distribution of Al in the interior of the Moon, to be 6 wt%. A Moon enriched in alumina was also found by Kuskov and Kronrod, who obtained an Al_2O_3 content of ~6 wt%. In relation to this, it might be remarked that the new value for the crustal thickness of 45 km [*Khan et al.*, 2000], comprising 7.6% of lunar volume, raises several questions, such as, how does it relate to the average crustal thickness and to the refractory element abundances in the whole Moon? If the new crustal thickness is extrapolated globally, an average thickness of around 52 km is found [*Wieczorek and Zuber*, 2004] (comprising about 8.7% of lunar volume). There is a trade-off as the plagioclase rich crust extends to a depth of 30 km [*Wieczorek and Zuber*, 2001], so that decreasing the

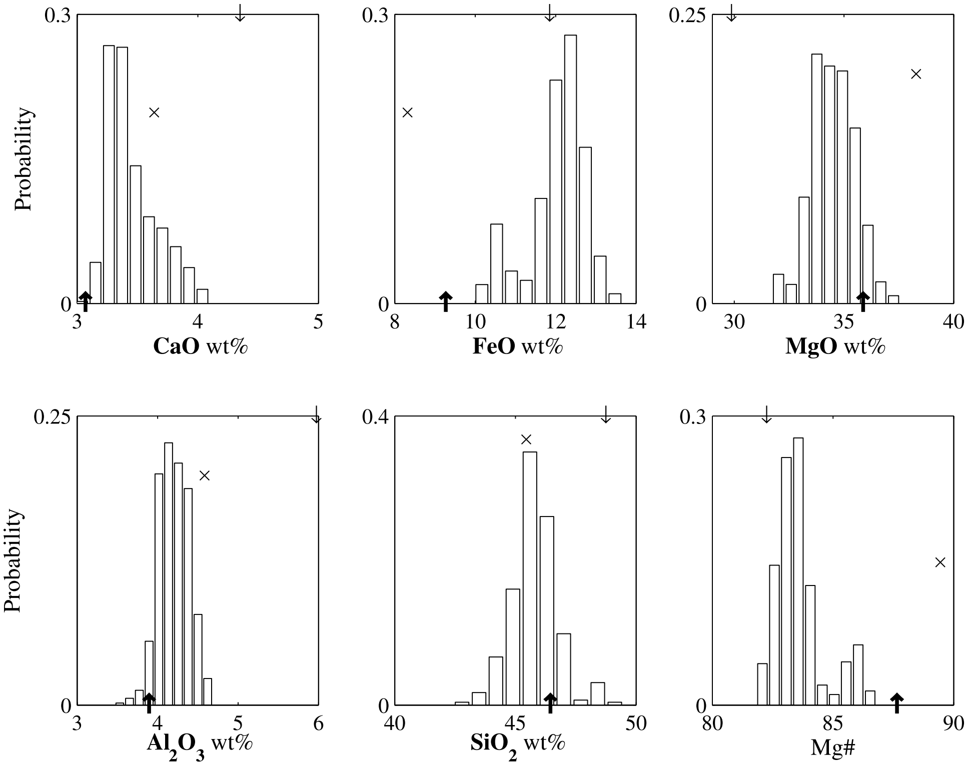

Figure 8. Marginal posterior *pdf*s displaying sampled bulk lunar compositions and Mg#s for the silicate part of the Moon (crust and mantle). Upward and downward pointing arrows indicate the bulk compositional estimates of *Warren* [2005] and *Kuskov and Kronrod* [1998] (model II), respectively, while crosses denote bulk composition of the Earth's upper mantle [*McDonough and Sun*, 1995].

crustal thickness will increase the relative proportions of the upper Al_2O_3-rich crust. If the crust is derived from a smaller volume of the Moon, then an increased bulk-Moon abundance of Al_2O_3 is required, which, incidentally is not necessarily indicated by the bulk compositions obtained here (Figure 8). Our results are indicative of refractory element abundances akin to those in the Earth's upper mantle (4.45 wt% [*McDonough and Sun*, 1995]) and as such lie in between the values obtained by *Taylor* [1982] and *Warren* [2005], whose preferred model (Mg/Si = 1.1× CI) has an Al_2O_3 abundance of 3.82 wt%.

[66] The compositional estimates of the upper mantle of the Earth [*McDonough and Sun*, 1995; *Salters and Stracke*, 2004] are principally based on studies of the composition of meteorites, mantle xenoliths and the basaltic products of mantle melting and are similar to Ringwood's pyrolite composition [*Ringwood*, 1966]. These compositions are able to reproduce the seismic velocity and density profiles of the Earth's upper mantle for likely geotherms [*Murakami and Yoshioka*, 2001] and are also in agreement with the radial electrical conductivity structure of the Earth [*Xu et al.*, 2000]. Moreover, and as already mentioned, they also have a sufficiently high Mg#, close to 0.9, to generate melts with a Mg# resembling the most primitive mid-ocean ridge basalts. The results of the present investigation generate mantle compositions for the Moon (Figure 6) that are different to that of pyrolite, as our models have higher FeO and lower MgO contents than the pyrolite composition, in general agreement with literature estimates (see Table 1). As concerns refractory lithophile element budgets, most of our models have slightly lower CaO and Al_2O_3 contents than pyrolite. Accordingly, our results are interpreted as implying compositional differences between the Earth and the Moon, contrary to the arguments of *Warren* [2005]. As discussed, lunar mantle Mg#s of approximately 0.83–0.84 found here match the observed Mg# of the most primitive mare basalts and are different from that of the Earth's (0.89), reflecting not only compositional differences but also different evolutionary histories for the upper mantles of the Earth and Moon.

7.3. Core

[67] Within the framework of the giant impact models, an iron core, if present, should be small. However, lunar formation models do not directly predict an iron core as outcome, they are merely compatible with the latter. Much has been said about the possible existence of a lunar core, whether of metallic or silicate composition, although a small (<1–3% by volume) iron or iron core possibly containing some light element such as S is currently favored. Most data, be they remotely sensed or gathered in situ, also seem to converge upon the necessity for a small lunar core with a radius <400 km of iron-like composition [e.g., *Hood and Jones*, 1987; *Mueller et al.*, 1988; *Hood et al.*, 1999; *Williams et al.*, 2001; *Righter*, 2002; *Wieczorek and Zuber*, 2002; *Khan et al.*, 2004; *Khan and Mosegaard*, 2005]. The reader is referred to, for example, *Hood and Zuber* [2000], *Williams et al.* [2001] and *Khan et al.* [2004] for further discussion on the lunar core.

[68] In spite of the fact that the core is not directly sensed by the seismic data and is most directly constrained by mass

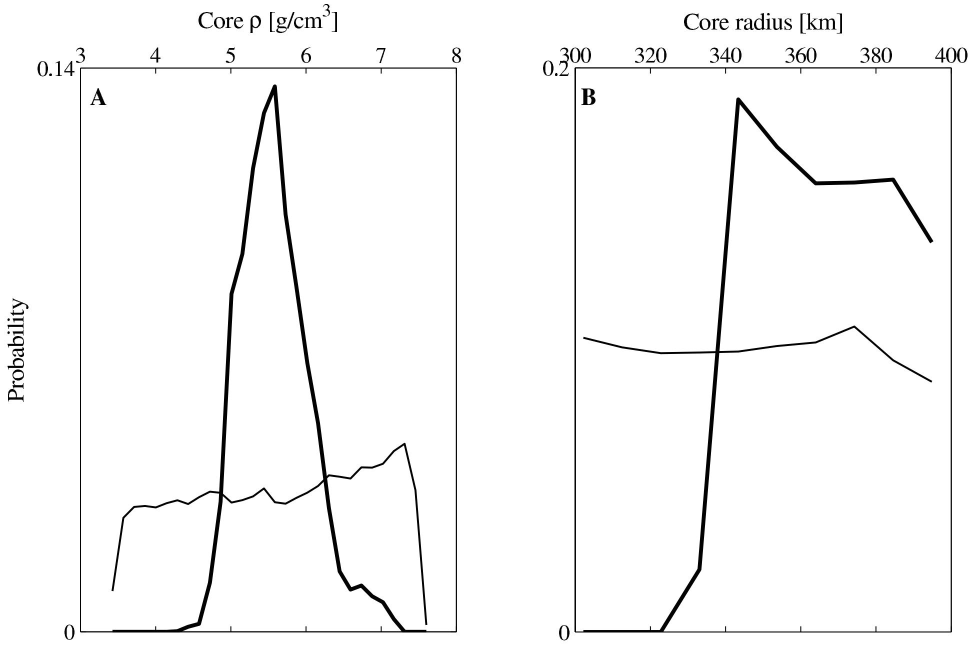

Figure 9. Prior (thin line) and posterior (thick line) *pdf*s showing sampled (a) core sizes and (b) densities. Results are in agreement with earlier inferences pointing to a small Fe core. The measured density for Fe-10wt%S at 1500°C and 5 GPa is 5.15 g/cm^3 [*Sanloup et al.*, 2000].

and moment of inertia, we can nonetheless use our results to place bounds on its size and state. The 1D marginal *pdf*'s (Figure 9), showing the distribution of sampled core densities and sizes reveal most probable values of $\rho \sim 5.5$ g/cm^3 and $r \sim 340$ km, respectively, in overall agreement with earlier assessments.

7.4. Implications for Lunar Structure, Origin, and Evolution

[69] Our inversion results indicate that the available seismic, mass and moment of inertia data can be modeled with a single homogeneous mantle composition that lies within the CFMAS system. However, the isotope geochemistry of mare basalts and picrite glasses indicate that compositional heterogeneity must be present within the mantle. This apparent paradox is also present on the Earth, where pyrolitic compositions give a good fit to spherically symmetric average velocity models for the upper mantle [e.g., *Cammarano et al.*, 2003], but isotopic compositions of mid-ocean ridge and ocean island basalts indicate that the upper mantle is variable on a number of length scales. In part, the paradox reflects the different length scales of sensitivity of the geophysical and geochemical sampling, where the seismic data are sensitive to long-wavelength variations, while the geochemistry of mantle melts may be influenced by the enhanced fusibility of small-scale heterogeneities in the mantle, which are known to be present on a length scale smaller than that of the melting region beneath mid-ocean ridges on earth. It is therefore encouraging, and perhaps fortuitous, that the mineralogy found in our inversion results is broadly consistent with the mineralogy of the lunar mantle inferred from the compositions of mare basalts and picrite glasses. This agreement also reflects the wide range of compositions that produce olivine, orthopyroxene, clinopyroxene and an aluminous phase in the CFMAS system.

[70] The initial interest in the bulk lunar composition was to test the hypothesis that the Moon was derived from the silicate mantle of the Earth, a notion dating back to George Darwin (1881) that resolved the difference in density between the two bodies. Although hotly debated following the Apollo sample return, the siren-like attractions of the model have diminished, despite the similarity in oxygen isotopes between the two bodies. This model has not survived the demonstration of significant differences (notably in FeO, MgO content) and the acceptance of the single impact hypothesis for lunar origin that derive ~80% of the Moon from the mantle of the impactor, not from the Earth.

[71] The enstatite chondrites indeed possess similar oxygen isotopic ratios to that of the Earth and Moon but have significant differences in major and volatile element concentrations that exclude them from consideration as possible building blocks. Given the wide variations among the major element compositions (Fe contents, Mg/Si and Al/Si ratios) and volatile element contents (e.g., higher K/U ratios) of chondritic meteorites and their differences from those of the Earth, it should not be surprising that the Moon also displays such differences.

[72] The bulk composition of the Moon can thus be understood within the general framework of the standard model for the origin of the inner solar system. All inner solar system bodies are strongly fractionated from the composition of the primordial rocky component of the solar nebula. Initial differences have been exacerbated by massive collisions that have produced such extremes as Mercury. The composition of the Moon thus represents one extreme in the compositions that result in that region from the stochastic assembly of planetary sized bodies from a hierarchy of smaller bodies. The bulk composition of the Moon is thus strongly fractionated from that of the initial nebula. It becomes a second order problem, that is only one

outcome among many other possibilities. Philosophically it points up the importance of such processes in the inner solar nebula, that lead to random outcomes. Such processes enhance the difficulties of constructing bodies similar to any of our inner planets in extrasolar planetary systems.

[73] Finally, we would like to point out that while the spread in major element abundances with depth is too great to provide useful constraints for geochemists and petrologists at present in order to test competing models for the origin and evolution of the Moon, the application of the procedure presented herein to refined seismic data from future missions can be expected to provide the clues needed to unravel these particular aspects. With respect to this, the identification of compositional zonation in the mantle, if present, is important as it provides a means to test models of lunar evolution that involve a magma ocean. Moreover, as part of this identification of zonation, it may be possible to search for the presence of the KREEP or ilmenite cumulate layer. However, in order to convert such new data into compositional structure, and to test for the presence of such layers, it will be necessary to incorporate the effect of elements like Ti, Cr, Na and K on the bulk physical properties. With this in mind, the acquisition of an improved lunar seismic data set, possibly from a global lunar seismic network [e.g., *Neal et al.*, 2004], cannot be stressed enough.

[74] **Acknowledgments.** We are grateful to L. Elkins-Tanton and K. Righter for constructive reviews. Comments by Y. Nakamura and M. Wieczorek as well as discussions with J. Longhi on an earlier version of this manuscript are also highly appreciated. A. Khan acknowledges support from the Carlsberg Foundation and the financial support provided through the European Community's Improving Human Potential Programme under contract RTN2-2001-00414, MAGE. J. Maclennan would like to thank NERC for funding (fellowship NER/I/S/2002/00609/2). This research was conducted in part at the Lunar and Planetary Institute, which is operated by the USRA under contract CAN-NCC5-679 with NASA. This is LPI contribution 1261.

References

Ahrens, L. H., and M. von Michaelis (1969), The composition of stony meteorites: V. Some aspects of the composition of the basaltic achondrites, *Earth Planet. Sci. Lett.*, *6*, 304.

Asimow, P. D., and J. Longhi (2004), The significance of multiple saturation points in the context of polybaric near-fractional melting, *J. Petrol.*, *45*, 2349.

Beard, B. L., L. A. Taylor, E. E. Scherer, C. M. Johnson, and G. A. Snyder (1998), The source region and melting mineralogy of high-titanium and low-titanium lunar basalts deduced from Lu-Hf isotope data, *Geochem. Cosmochim. Acta*, *62*, 525.

Beck, A. R., Z. T. Morgan, Y. Liang, and P. C. Hess (2006), Dunite channels as viable pathways for mare basalt transport in the deep lunar mantle, *Geophys. Res. Lett.*, *33*, L01202, doi:10.1029/2005GL024008.

Bills, B. G., and A. J. Ferrari (1977), A lunar density model consistent with topographic, gravitational, librational, and seismic data, *J. Geophys. Res.*, *82*, 1306.

Binder, A. B., and M. Lange (1980), On the thermal history, thermal state, and related tectonism of a Moon of fission origin, *J. Geophys. Res.*, *85*, 3194.

Buck, W. R., and M. N. Toksöz (1980), The bulk composition of the Moon based on geophysical constraints, *Proc. Lunar Planet. Sci. Conf., 11th*, 2043.

Cameron, A. G. W. (2000), Higher resolution simulations of the giant impact, in *Origin of the Earth and Moon*, edited by R. M. Canup and K. Righter, p. 133, Univ. of Ariz. Press, Tucson.

Cameron, A. G. W., and W. R. Ward (1976), The origin of the Moon, *Proc. Lunar Sci. Conf., VIIth*, 120.

Cammarano, F., S. Goes, P. Vacher, and D. Giardini (2003), Inferring upper-mantle temperatures from seismic velocities, *Phys. Earth. Planet. Inter.*, *138*, 197.

Canup, R. M. (2004), Simulations of a late lunar-forming impact, *Icarus*, *168*, 433.

Canup, R. M., and E. Asphaug (2001), Origin of the Moon in a giant impact near the end of the Earth's formation, *Nature*, *412*, 708.

Conel, J. E., and J. B. Morton (1975), Interpretation of lunar heat flow data, *Moon*, *14*, 263.

Connolly, J. A. D. (2005), Computation of phase equilibria by linear programming: A tool for geodynamic modeling and an application to subduction zone decarbonation, *Earth Planet. Sci. Lett.*, *236*, 524.

Connolly, J. A. D., and D. M. Kerrick (2002), Metamorphic controls on seismic velocity of subducted oceanic crust at 100–250 km depth, *Earth Planet. Sci. Lett.*, *204*, 61.

Davis, P. A., and P. D. Spudis (1985), Petrologic province maps of the lunar highlands derived from orbital geochemical data, *Proc. Lunar Planet. Sci. Conf. 16th*, Part 1, *J. Geophys. Res.*, *90*, suppl., D61.

Delano, J. W. (1986), Abundances of cobalt, nickel and volatiles in the silicate portion of the Moon, in *Origin of the Moon*, edited by W. K. Hartmann, R. J. Phillips, and G. J. Taylor p. 231, Lunar Planet. Inst., Houston, Tex.

Drake, M. J. (1996), Geochemical constraints on the origin of the Moon: Abundance of U, *Meteorit. Planet. Sci.*, *31*, A38.

Drake, M. J., and K. Righter (2002), Determining the composition of the Earth, *Nature*, *416*, 39.

Draper, D. S., S. A. Dufrane, and C. K. Shearer (2004), Preliminary high pressure phase relations of Apollo 15 green C glass: Assessment of the role of garnet, *Lunar Planet. Sci.* [CD-ROM], *XXXVth*, abstract 1297.

Duba, A., H. C. Heard, and R. N. Schock (1976), Electrical conductivity of orthopyroxene to 1400°C and the resulting selenotherm, *Proc. Lunar. Sci. Conf., 7th*, 3173.

Dyal, P., C. W. Parkin, and W. D. Daily (1976), Structure of the lunar interior from magnetic field measurements, *Proc. Lunar Sci. Conf., 7th*, 3077.

Elkins-Tanton, L. T., N. Chatterjee, and T. L. Grove (2003), Experimental and petrological constraints on lunar differentiation from the Apollo 15 green picritic glasses, *Meteorit. Planet. Sci.*, *38*, 515.

Ghiorso, M. S., and R. O. Sack (1995), Chemical mass-transfer in magmatic processes: 4. A revised and internally consistent thermodynamic model for the interpolation and extrapolation of liquid-solid equilibria, in *Magmatic Systems at Elevated Temperatures and Pressures*, *Contrib. Mineral. Petrol.*, *119*, 197.

Ghiorso, M. S., M. M. Hirschmann, P. W. Reiners, and V. C. Kress (2002), The pMELTS: A revision of MELTS for improved calculation of phase relations and major element partitioning related to partial melting of the mantle to 3 GPa, *Geochem. Geophys. Geosyst.*, *3*(5), 1030, doi:10.1029/2001GC000217.

Goins, N. R., M. N. Toksoz, and A. M. Dainty (1978), Seismic structure of the lunar mantle—An overview, *Proc. Lunar Planet. Sci. Conf. 9th*, 3575.

Goins, N. R., A. M. Dainty, and M. N. Toksöz (1981), Lunar seismology: The internal structure of the Moon, *J. Geophys. Res.*, *86*, 5061.

Hartmann, W. K., and D. R. Davis (1975), Satellite-sized planetesimals and lunar origin, *Icarus*, *24*, 504.

Haskin, L. A. (1998), The Imbrium impact event and the thorium distribution at the lunar highlands surface, *J. Geophys. Res.*, *103*, 1679.

Hess, P. C. (1994), Petrogenesis of lunar troctolites, *J. Geophys. Res.*, *99*, 19,083.

Hess, P. C., and E. M. Parmentier (1995), A model for the thermal and chemical evolution of the Moon's interior: Implications for the onset of mare volcanism, *Earth Planet. Sci. Lett.*, *134*, 501.

Hirschmann, M. (2000), Mantle solidus: Experimental constraints and the effects of peridotite composition, *Geochem. Geophys. Geosyst.*, *1*, doi:10.1029/2000GC000070.

Hobbs, B. A., L. L. Hood, F. Herbert, and C. P. Sonett (1983), An upper bound on the radius of a highly electrically conducting lunar core, *J. Geophys. Res.*, *88*, Suppl., B97.

Hood, L. L. (1986), Geophysical constraints on the interior of the Moon, in *Origin of the Moon*, edited by W. K. Hartmann, R. J. Phillips, and G. J. Taylor, p. 361, Lunar Planet. Inst., Houston, Tex.

Hood, L. L., and J. H. Jones (1987), Geophysical constraints on lunar bulk composition and structure: A reassessment, *J. Geophys. Res.*, *92*, 396.

Hood, L. L., and M. T. Zuber (2000), Recent refinements in geophysical constraints on lunar origin and evolution, in *Origin of the Earth and Moon*, edited by R. M. Canup and K. Righter, p. 397, Univ. of Ariz. Press, Tucson.

Hood, L. L., F. Herbert, and C. P. Sonett (1982a), The deep lunar electrical conductivity profile: Structural and thermal inferences, *J. Geophys. Res.*, *87*, 5311.

Hood, L. L., F. Herbert, and C. P. Sonett (1982b), Further efforts to limit lunar internal temperatures from electrical conductivity determinations, *J. Geophys. Res.*, *87*, Suppl., A109.

Hood, L. L., D. L. Mitchell, R. P. Lin, M. H. Acuna, and A. B. Binder (1999), Initial measurements of the lunar-induced magnetic dipole moment using lunar prospector magnetometer data, *Geophys. Res. Lett.*, *26*, 2327.

Huebner, J. S., L. B. Wiggins, and A. Duba (1979), Electrical conductivity of pyroxene which contains trivalent cations: Laboratory measurements and the lunar temperature profile, *J. Geophys. Res.*, *84*, 4652.

Jarosewich, E. (1990), Chemical analyses of meteorites: A compilation of stony and iron meteorite analyses, *Meteoritics*, *25*, 323.

Jolliff, B. L., J. J. Gillis, L. A. Haskin, R. L. Korotev, and M. A. Wieczorek (2000), Major crustal terranes: Surface expressions and crust-mantle origins, *J. Geophys. Res.*, *105*, 4197.

Jones, J. H., and J. W. Delano (1989), A three-component model for the bulk composition of the Moon, *Geochem. Cosmochim. Acta*, *53*, 513.

Jones, J. H., and L. L. Hood (1990), Does the Moon have the same chemical composition as the Earth's upper mantle, in *Origin of the Earth*, edited by H. E. Newsom and J. H. Jones, p. 85, Lunar Planet. Inst., Houston, Tex.

Jones, J. H., and H. Palme (2000), Geochemical constraints on the origin of the Earth and Moon, in *Origin of the Earth and Moon*, edited by R. M. Canup and K. Righter, p. 197, Univ. of Ariz. Press, Tucson.

Karato, S. (1993), Importance of anelasticity in the interpretation of seismic tomography, *Geophys. Res. Lett.*, *20*, 1623.

Kelemen, P. B., G. Hirth, N. Shimizu, M. Spiegelman, and H. J. B. Dick (1997), A review of melt migration processes in the adiabatically upwelling mantle beneath oceanic spreading ridge, *Philos. Trans. R. Soc., Ser. A*, *355*, 283.

Kesson, S. E., and A. E. Ringwood (1976), Mare basalt petrogenesis in a dynamic moon, *Earth Planet. Sci. Lett.*, *30*, 155.

Khan, A., and K. Mosegaard (2002), An inquiry into the lunar interior: A nonlinear inversion of the Apollo lunar seismic data, *J. Geophys. Res.*, *107*(E6), 5036, doi:10.1029/2001JE001658.

Khan, A., and K. Mosegaard (2005), Further constraints on the deep lunar interior, *Geophys. Res. Lett.*, *32*, L22203, doi:10.1029/2005GL023985.

Khan, A., K. Mosegaard, and K. L. Rasmussen (2000), A new seismic velocity model for the Moon from a Monte Carlo inversion of the Apollo lunar seismic data, *Geophys. Res. Lett.*, *27*, 1591.

Khan, A., K. Mosegaard, J. G. Williams, and P. Lognonné (2004), Does the Moon possess a molten core? Probing the deep lunar interior using results from LLR and Lunar Prospector, *J. Geophys. Res.*, *109*, E09007, doi:10.1029/2004JE002294.

Khan, A., J. A. D. Connolly, J. Maclennan, and K. Mosegaard (2006), Joint inversion of seismic and gravity data for lunar composition and thermal state, *Geophys. J. Int.*, in press.

Konopliv, A., A. B. Binder, L. L. Hood, A. B. Kucinskas, W. L. Sjögren, and J. G. Williams (1998), Improved gravity field of the Moon from Lunar Prospector, *Science*, *281*, 1476.

Korotev, R. L. (2000), The great lunar hot spot and the composition and origin of the Apollo mafic ("LKFM") impact-melt breccias, *J. Geophys. Res*, *105*, 4317.

Kuskov, O. L. (1997), Constitution of the Moon: 4. Composition of the mantle from seismic data, *Phys. Earth Planet. Inter.*, *102*, 239.

Kuskov, O. L., and V. A. Kronrod (1998), Constitution of the Moon: 5. Constraints on density, temperature and radius of a core, *Phys. Earth Planet. Inter.*, *107*, 285.

Kuskov, O. L., and V. A. Kronrod (2001), Core sizes and internal structure of the Earth's and Jupiter's satellites, *Icarus*, *151*, 204.

Kuskov, O. L., V. A. Kronrod, and L. L. Hood (2002), Geochemical constraints on the seismic properties of the lunar mantle, *Phys. Earth Planet. Inter.*, *134*, 175.

Langseth, M. G., S. J. Keihm, and K. Peters (1976), Revised lunar heat-flow values, *Proc. Lunar Sci. Conf., 7th*, 3143.

Latham, G. V., M. Ewing, F. Press, and G. Sutton (1969), Apollo passive seismic experiment, *Science*, *165*, 241.

Latham, G. V., M. Ewing, R. Press, G. Sutton, J. Dorman, Y. Nakamura, M. N. Toksöz, R. Wiggins, J. Derr, and F. Duennebier (1970), Passive seismic experiment, *Science*, *167*, 455.

Lodders, K., and B. Fegley (1998), *The Planetary Scientist's Companion*, Oxford Univ. Press, New York.

Lognonné, P., J. Gagnepain-Beyneix, and H. Chenet (2003), A new seismic model of the Moon: Implications for structure, thermal evolution and formation of the Moon, *Earth Planet. Sci. Lett.*, *211*, 27.

Longhi, J. (1977), Magma oceanography: 2. Chemical evolution and crustal formation, *Proc. Lunar Sci. Conf., 8th*, 600.

Longhi, J. (1992a), Experimental petrology and petrogensis of mare volcanic glasses, *Geochem. Cosmochim. Acta*, *56*, 2235.

Longhi, J. (1992b), Origin of picritic green glass magmas by polybaric fractional fusion, *Proc. Lunar Planet. Sci. Conf., 22nd*, 343.

Lucey, P., G. J. Taylor, and E. Malaret (1995), Abundance and distribution of iron on the Moon, *Science*, *268*, 1150.

McDonough, W. F., and S. S. Sun (1995), The composition of the Earth, *Chem. Geol.*, *120*(3–4), 223.

Minster, J. B. (1980), Anelasticity and attenuation, in *Physics of the Earth's Interior: Proceedings of the International School of Physics "Enrico Fermi"*, edited by A. M. Dziewonski and E. Boschi, p. 152, Elsevier, New York.

Morgan, J. W., J. Hertogen, and E. Anders (1978), The Moon: Composition determined by nebular processes, *Moon Planets*, *18*, 465.

Mosegaard, K., and A. Tarantola (1995), Monte Carlo sampling of solutions to inverse problems, *J. Geophys. Res.*, *100*, 12,431.

Mueller, S., G. J. Taylor, and R. J. Phillips (1988), Lunar composition: A geophysical and petrological synthesis, *J. Geophys. Res.*, *93*, 6338.

Murakami, T., and S. Yoshioka (2001), The relationship between the physical properties of the assumed pyrolite composition and depth distributions of seismic velocities in the upper mantle, *Earth Planet. Sci. Lett.*, *125*, 1.

Nakamura, Y. (1983), Seismic velocity structure of the lunar mantle, *J. Geophys. Res.*, *88*, 677.

Nakamura, Y. (2005), Farside deep moonquakes and deep interior of the Moon, *J. Geophys. Res.*, *110*, E01001, doi.10.1029/2004JE002332.

Nakamura, Y., and J. Koyama (1982), Seismic Q of the lunar upper mantle, *J. Geophys. Res.*, *87*, 4855.

Nakamura, Y., D. Lammlein, G. V. Latham, M. Ewing, J. Dorman, F. Press, and M. N. Toksöz (1973), New seismic data on the state of the deep lunar interior, *Science*, *181*, 49.

Nakamura, Y., G. V. Latham, and J. Dorman (1980), How we processed Apollo lunar seismic data, *Phys. Earth Planet Inter.*, *21*, 218.

Nakamura, Y., G. V. Latham, and J. Dorman (1982), Apollo Lunar Seismic Experiment: Final summary, *J. Geophys. Res.*, *87*, suppl., A117.

Neal, C. R. (2001), Interior of the Moon: The presence of garnet in the primitive deep lunar mantle, *J. Geophys. Res.*, *106*, 27,865.

Neal, C. R., et al. (2004), The Lunar Seismic Network: Mission update, *Lunar Planet. Sci.* [CD-ROM], *XXXVth*, abstract 2093.

Newsom, H. E. (1986), Constraints on the origin of the Moon from the abundance of molybdenum and other siderophile elements, in *Origin of the Moon*, edited by W. K. Hartmann, R. J. Phillips, and G. J. Taylor, p. 203, Lunar Planet. Inst., Houston, Tex.

O'Neill, H. S. C. (1991), The origin of the Moon and the early history of the Earth—A chemical model: Part I. The Moon, *Geochem. Cosmochim. Acta*, *55*, 1135.

Palme, H., and K. G. Nickel (1985), Ca/Al ratio and composition of the Earth's upper mantle, *Geochem. Cosmochim. Acta*, *49*, 2123.

Prettyman, T. H., W. C. Feldman, D. J. Lawrence, G. W. McKinney, A. B. Binder, R. C. Elphic, O. M. Gasnault, S. Maurice, and K. R. Moore (2002), Library least squares analysis of Lunar Prospector gamma ray spectra, *Lunar Planet. Sci.* [CD-ROM], *XXXIIIrd*, abstract 2012.

Pullan, S., and K. Lambeck (1980), On constraining lunar mantle temperatures from gravity data, *Proc. Lunar Planet. Sci. Conf., 11th*, 2031.

Rasmussen, K. L., and P. H. Warren (1985), Megaregolith thickness, heat flow, and the bulk composition of the moon, *Nature*, *313*, 121.

Righter, K. (2002), Does the Moon have a metallic core? Constraints from giant-impact modelling and siderophile elements, *Icarus*, *158*, 1.

Righter, K., and M. J. Drake (1996), Core formation in Earth's Moon, Mars, and Vesta, *Icarus*, *124*, 512.

Righter, K., R. J. Walker, and P. H. Warren (2000), Significance of highly siderophile elements and osmium isotopes in the lunar and terrestrial mantles, in *Origin of the Earth and Moon*, edited by R. M. Canup and K. Righter, p. 291, Univ. of Ariz. Press, Tucson.

Ringwood, A. E. (1966), Mineralogy of the mantle, in *Advances in Earth Science*, edited by P. Hurley, p. 357, MIT Press, Cambridge, Mass.

Ringwood, A. E. (1979), *Origin of the Earth and Moon*, Springer, New York.

Ryder, G., and P. Spudis (1987), Chemical composition and origin of Apollo 15 impact melts, *Proc. Lunar Planet. Sci. Conf., 17th*, Part 2, *J. Geophys. Res.*, *92*, suppl., E432.

Salters, V. J. M., and A. Stracke (2004), Composition of the depleted mantle, *Geochem. Geophys. Geosyst.*, *5*, Q05B07, doi:10.1029/2003GC000597.

Sanloup, C., F. Guyot, P. Gillet, G. Fiquet, M. Mezouar, and I. Martinez (2000), Density measurements of liquid Fe-S alloys at high pressure, *Geophys. Res. Lett.*, *27*, 811.

Schubert, G., R. E. Young, and P. Cassen (1977), Subsolidus convection models of the lunar internal temperature, *Philos. Trans. R. Soc., Ser. A.*, *285*, 523.

Shearer, C. K., and J. J. Papike (1993), Basaltic magmatism on the Moon: A perspective from volcanic picritic glass beads, *Geochem. Cosmochim. Acta*, *57*, 4785.

Smith, D. E., M. T. Zuber, G. A. Neumann, and F. G. Lemoine (1997), Topography of the Moon from the Clementine LIDAR, *J. Geophys. Res.*, *102*, 1591.

Smith, P. M., and P. D. Asimow (2005), Adiabat_1ph: A new public front-end to the MELTS, pMELTS, and pHMELTS models, *Geochem. Geophys. Geosyst.*, *6*, Q02004, doi:10.1029/2004GC000816.

Snyder, G. A., L. A. Taylor, and C. R. Neal (1992), A chemical model for generating the sources of mare basalts: Combined equilibrium and fractional crystallisation of the lunar magmasphere, *Geocim. Cosmochim. Acta*, *56*, 3809.

Solomon, S. C., and J. Chaiken (1976), Thermal expansion and thermal stress in the Moon and terrestrial planets: Clues to early thermal history, *Proc. Lunar Sci. Conf., 7th*, 3229.

Sonett, C. P. (1982), Electromagnetic induction in the Moon, *Rev. Geophys.*, *20*, 411.

Spudis, P., B. R. Hawke, and P. Lucey (1984), Composition of Orientale basin deposits and implications for the lunar basin-forming process, *Proc. Lunar Planet. Sci. Conf. 15th*, Part 1, *J. Geophys. Res.*, *89*, suppl., C197.

Stevenson, D. J. (1990), Fluid dynamics of core formation, in *Origin of the Earth*, edited by H. E. Newsom and J. H. Jones, p. 231, Oxford Univ. Press, New York.

Tarantola, A. (1987), *Inverse Problem Theory*, Elsevier Sci., New York.

Tarantola, A., and B. Valette (1982), Inverse problems: Quest for information, *J. Geophys.*, *50*, 159.

Tatsumoto, M., W. R. Premo, and D. M. Unruh (1987), Origin of lead from green glass of Apollo 15426: A search for primitive lunar lead, *Proc. Lunar Planet. Sci. Conf. 17th*, Part 2, *J. Geophys. Res.*, *92*, suppl., E361.

Taylor, L. A., G. J. Taylor, and S. R. Taylor (2006), The Moon: A Taylor perspective, *Geochem. Cosmochim. Acta*, in press.

Taylor, S. R. (1982), *Planetary Science: A Lunar Perspective*, Lunar Planet. Inst., Houston, Tex.

Taylor, S. R. (1986), The origin of the Moon: Geochemical considerations, in *Origin of the Moon*, edited by W. K. Hartmann, R. J. Phillips, and G. J. Taylor, p. 125, Lunar Planet. Inst., Houston, Tex.

Taylor, S. R. (2001), *Solar System Evolution: A New Perspective*, 2nd ed., Cambridge Univ. Press, New York.

Taylor, S. R., and P. Jakes (1974), The geochemical evolution of the Moon, *Proc. Lunar Sci. Conf., 5th*, 1287.

Toksöz, M. N. (1974), Geophysical data and the interior of the Moon, *Annu. Rev. Earth Planet. Sci.*, *2*, 151.

Toksöz, M. N., A. M. Dainty, S. C. Solomon, and K. R. Anderson (1974), Structure of the Moon, *Rev. Geophys.*, *12*, 539.

Toksöz, M. N., A. T. Hsui, and D. H. Johnston (1978), Thermal evolutions of the terrestrial planets, *Moon Planets*, *18*, 281.

Vacher, P., A. Mocquet, and C. Sotin (1998), Computation of seismic profiles from mineral physics: The importance of the non-olivine components for explaining the 660 km depth discontinuity, *Earth Planet. Sci. Lett.*, *106*, 275.

Wänke, H., and G. Dreibus (1986), Geochemical evidence for the formation of the Moon by impact-induced fission of the proto-Earth, in *Origin of the Moon*, edited by W. K. Hartmann, R. J. Phillips, and G. J. Taylor, p. 361, Lunar Planet. Inst., Houston, Tex.

Wänke, H. et al. (1977), On the chemistry of the lunar samples and achondrites—Primary matter in the lunar highlands: A reevaluation, *Proc. Lunar Sci. Conf., 8th*, 2191.

Warren, P. H. (1985), The magma ocean concept and lunar evolution, *Annu. Rev. Earth Planet. Sci.*, *13*, 201.

Warren, P. H. (1986), The bulk-Moon MgO/FeO ratio: A highlands perspective, in *Origin of the Moon*, edited by W. K. Hartmann, R. J. Phillips, and G. J. Taylor, p. 125, Lunar Planet. Inst., Houston, Tex.

Warren, P. H. (2005), "New" lunar meteorites: II. Implications for composition of the global lunar surface, lunar crust, and the bulk Moon, *Meteorit. Planet. Sci.*, *40*, 1.

Warren, P. H., and G. W. Kallemeyn (1984), Pristine rocks (8th Foray): "Plagiophile" element ratios, crustal genesis, and the bulk composition of the moon, *J. Geophys. Res.*, *89*, suppl., C16.

Warren, P. H., and K. L. Rasmussen (1987), Megaregolith insulation, internal temperatures, and bulk uranium content of the Moon, *J. Geophys. Res.*, *92*, 3453.

Watt, J. P., G. F. Davies, and R. J. O'Connell (1976), The elastic properties of composite minerals, *Rev. Geophys.*, *14*, 541.

Wieczorek, M. A. (2003), The thickness of the lunar crust: How low can you go?, *Lunar Planet. Sci.* [CD-ROM], *XXXIV*, abstract 1330.

Wieczorek, M. A., and R. J. Philipps (2000), The "Procellarum KREEP Terrane": Implications for mare volcanism and lunar evolution, *J. Geophys. Res.*, *105*, 20,417.

Wieczorek, M. A., and M. T. Zuber (2001), The composition and origin of the lunar crust: Constraints from central peaks and crustal thickness modeling, *Geophys. Res. Lett.*, *28*, 4023.

Wieczorek, M. A., and M. T. Zuber (2002), The "core" of the Moon: Iron or titanium rich?, *Lunar Planet. Sci.* [CD-ROM], *XXXIII*, abstract 1384.

Wieczorek, M. A., and M. T. Zuber (2004), Improved constraints from geoid-to-topography ratios, *J. Geophys. Res.*, *109*, E01009, doi:10.1029/2003JE002153.

Wieczorek, M. A., B. L. Jolliff, J. J. Gillis, L. L. Hood, K. Righter, A. Khan, M. E. Pritchard, B. P. Weiss, S. Thompkins, and J. G. Williams (2006), The constitution and structure of the lunar interior, *New Views of the Moon*, in press.

Williams, J. G., D. H. Boggs, C. F. Yoder, J. T. Radcliff, and J. O. Dickey (2001), Lunar rotational dissipation in solid body and molten core, *J. Geophys. Res.*, *106*, 27,933.

Wood, J. (1986), Moon over Mauna Loa: A review of hypotheses of formation of Earth's Moon, in *Origin of the Moon*, edited by W. K. Hartmann, R. J. Phillips, and G. J. Taylor, p. 12, Lunar Planet. Inst., Houston, Tex.

Xu, Y. S., T. J. Shankland, and B. T. Poe (2000), Laboratory-based electrical conductivity in the Earth's mantle, *J. Geophys. Res.*, *105*, 27,865.

J. A. D. Connolly, Earth Sciences Department, Swiss Federal Institute of Technology, Soneggstrasse 5, CH-8092 Zurich, Switzerland. (james.connolly@erdw.ethz.ch)

A. Khan, Niels Bohr Institute, University of Copenhagen, Juliane Maries Vej 30, DK-2100 Copenhagen, Denmark. (amir@gfy.ku.dk)

J. Maclennan, Department of Earth Sciences, University of Cambridge, Downing Street, Cambridge CB2 3EQ, UK. (john.maclennan@glg.ed.ac.uk)

S. R. Taylor, Department of Earth and Marine Sciences, Australian National University, Canberra ACT 0200, Australia. (ross.taylor@anu.edu.au)